C.P. No. 1326



PROCUREMENT EXECUTIVE, MINISTRY OF DEFENCE

*AERONAUTICAL RESEARCH COUNCIL*

*CURRENT PAPERS*

# Low-Speed Wind-Tunnel Tests of a Two-Dimensional Wing fitted with Two Plain Differentially-Deflected Trailing-Edge Flaps

*by*

*John Mckie*

*Aerodynamics Dept., R.A.E., Farnborough*

LONDON: HER MAJESTY'S STATIONERY OFFICE

1975

PRICE £1-80 NET

UDC 533.695.16 : 533.694.2 : 533.6.048.2

*CP No.1326
December 1974

# LOW-SPEED WIND-TUNNEL TESTS OF A TWO-DIMENSIONAL WING FITTED WITH TWO PLAIN, DIFFERENTIALLY-DEFLECTED, TRAILING-EDGE FLAPS

by

John McKie

## SUMMARY

Chordwise pressure distributions were measured at several spanwise stations on a two-dimensional model wing fitted with a plain-hinged, trailing-edge flap, at a Reynolds number of $1.9 \times 10^6$ based on chord. The flap was divided into two parts and was deflected to a maximum of $5^\circ$. When the flaps were deflected differentially, the transition from a pressure distribution characteristic of the flaps-deflected configuration, to one characteristic of the flaps-up situation, took place within a spanwise distance of about 10% of the chord. This length was independent of the angle of incidence. Integrations for sectional normal force indicated, however, that modifications to the local circulation caused by a discontinuity in angle of flap deflection were apparent more than one chord distance away from the flap junction.

---

* Replaces RAE Technical Report 74174 - ARC 35971

## CONTENTS


| | | Page |
|---|---|---|
| 1 | INTRODUCTION | 3 |
| 2 | DETAILS OF THE MODEL AND DATA-LOGGING SYSTEM | 3 |
| | 2.1 The model | 3 |
| | 2.2 Data-logging system | 6 |
| 3 | DESCRIPTION OF THE TESTS | 6 |
| | 3.1 Wind-tunnel runs | 6 |
| | 3.2 Corrections and accuracy | 8 |
| | 3.3 Repeatability | 9 |
| 4 | RESULTS | 10 |
| 5 | CONCLUSIONS | 14 |
| Table 1 | Coordinates of the aerofoil section | 16 |
| Table 2 | Positions of chordwise rows of pressure holes | 17 |
| Table 3 | Coordinates of the auxiliary pressure holes | 17 |
| Symbols | | 18 |
| References | | 19 |
| Illustrations | | Figures 1-19 |
| Detachable abstract cards | | - |

## 1 INTRODUCTION

The experiments reported here form part of a programme to investigate part-span-flap effects and to develop methods for their prediction. In a linear theory developed by the author[1,2], it is assumed that the chordwise pressure distribution changes discontinuously in the spanwise direction across a flap junction. That is to say, at an infinitesimal spanwise distance from the junction, on the deflected side the chordwise pressure distribution is typical of that for a flapped aerofoil section, and on the other side it is typical of that for a section without a flap. During some experiments[3] on a rectangular wing of aspect ratio 7 and 254mm chord fitted with part-span flaps, the opportunity was taken to investigate the truth of this assumption. Chordwise pressure distributions were obtained at short distances either side of a discontinuity in flap deflection. For a flap angle of $20^{\circ}$, the results showed that the chordwise pressure distribution changed from the one type to the other in a distance equal to about 30% of the chord. Although this distance could be considered 'short' on such a high-aspect-ratio wing, the model was not ideal for detailed investigations of the pressure distribution and the results could not be used to justify the theoretical model.

This Report describes experiments of a similar kind, but on a model designed specifically for the purpose of obtaining detailed information about the distribution of pressure on a wing with a part-span flap. The tests were conducted on a model wing of 457mm chord, mounted vertically between the floor and roof of a wind tunnel. The floor and roof boundary layers in the vicinity of the junctions with the wing were removed by suction to ensure two-dimensional flow conditions. The wing had a simple trailing-edge flap divided into two portions which could be deflected differentially. In order to minimise the amount of separated flow, the flaps were deflected a maximum of $5^{\circ}$ in these experiments. The results are presented in the form of chordwise pressure distributions and spanwise variations of local normal-force coefficient.

## 2 DETAILS OF THE MODEL AND DATA-LOGGING SYSTEM

### 2.1 The model

The aerofoil had a chord of 457 mm and was 2.743 m in length, to fit between the floor and roof turntables of the 13ft × 9ft low-speed wind tunnel at RAE Bedford (see Fig.1). The model was constructed of glass cloth and epoxy resin on a steel core in four major components: detachable leading and trailing edges, a centre assembly and a blowing tube. The aerofoil profile was similar

to that used by Foster *et al*[4] (RAE 2815), and the section coordinates are given in Table 1. Inserts were manufactured to fit between the leading edge and the centre assembly, in order to give the nose varying amounts of deflection. None of these inserts were used in the experiments reported here.

The trailing edge formed a simple plain flap and was designed to rotate about a circular tube (the blowing tube) attached to the centre assembly (see Fig.2). It was originally intended to control the boundary layer on the upper surface of the flap by injecting compressed air into it from a slot at the flap knuckle. It was hoped thus to maintain attached flow at the trailing edge for angles of deflection up to $80^{\circ}$. The slot was of constant width across the span of the wing and was formed between the blowing tube and the lower lip of the jet deflector. This deflector was a spanwise steel strip attached to the blowing tube and its upper surface formed part of the aerofoil section profile. The underside of the deflector was hollow, to enclose a plenum chamber behind the slot. Air passed to this chamber from the blowing tube via a number of small holes in the tube wall. The spacing of these holes decreased towards the centre of the wing in an attempt to obtain a uniform spanwise distribution of blowing air. However, calibration tests of the blowing slot indicated that the momentum of the blowing jet at the exit of the slot was so far from being uniform along its length that the requirement for two-dimensional flow over the wing would necessitate extensive modification of the rig. As a result, the idea of using this method to provide boundary-layer control by blowing had to be dropped for this series of tests and a dummy blowing tube and deflector were built. During the experiments, the angle of flap deflection was limited to $5^{\circ}$ in order to avoid separation of the flow at the trailing edge.

The trailing-edge flap was split into two parts (port and starboard flaps, see Fig.1) at a distance of 152mm below the centreline of the tunnel. The flap hinge was at the centre of the blowing tube, which was at the 70% chord position and 0.7% chord above the chordline. Each flap was attached to the centre assembly by three brackets and to the blowing tube by a number of locking screws (see Figs.1 and 2). The inner faces of the flaps were circular cylindrical, in order to slide around the blowing tube. The junctions of these faces with the upper and lower surfaces were thin cusps. As originally manufactured, both surfaces were made entirely of resin with the result that the lips were very fragile. However, it was also found that the upper lip was distorted and it was impossible to sit it properly onto the blowing tube along the whole of its length. A consequence was that the flow over the flap knuckle was seriously disturbed and

on some parts of the wing was completely separated over the whole of the flap chord. It was therefore decided to remove the upper lip and rebate the flap down to its steel core. A new lip was manufactured of spring steel with a finely-honed edge which could be sprung onto the blowing tube by means of the attachment screws (see Fig.2).

Fig.1 shows the main areas of the wing fitted with surface-pressure tubes. These areas extended from the flap break to 72% chord to port and from 72% to 94% chord distance from the flap break on the starboard side. The tubes ran in the spanwise direction, 41 on the upper surface and 31 on the lower. The mean coordinates of the pressure holes in the tubes are listed in Table 1. Chordwise pressure distributions could be obtained at 15 stations, 12 in the main area and three on the narrow area on the starboard part of the wing. The distances of these stations from the flap break, made non-dimensional on wing chord, are listed in Table 2. Station 12 was at the flap break and had, of course, no surface-pressure holes on the flap. As can be seen from Fig.1, stations 1 to 12 covered an area symmetric about the centreline of the tunnel, so that with the two flaps deflected equally, the symmetry of the flow could be assessed. Also rows 1 and 13 were equidistant from the flap break, so that again flow symmetry could be examined.

In order to ensure that changes in the chordwise pressure distributions with distance from the discontinuity in angle of flap deflection were not in part due to flow irregularities which would be present with the flaps equally deflected, it was important to maintain two-dimensional flow conditions over as large a part of the model as possible. This was accomplished by using the suction method of Foster and Lawford[5] to remove parts of the boundary layers on the wind-tunnel roof and floor at the junctions with the wing. The suction boxes, set flush into the turntables, were those used previously by Foster *et al*[4] but with their tunnel-side surfaces replaced by ones designed for the present model. The boundary layers were sucked through holes in these surfaces, 4.3 mm in diameter, placed at 12.7mm intervals 6.4mm outside the contour of the wing. The holes not required for a particular flap angle were sealed with adhesive tape. The amounts of suction applied to the two boxes could be controlled independently, up to a combined total of 2.6 $m^3/s$ at 1 bar. The levels of suction were kept the same in each box.

The effect of the suction was monitored by the behaviour of tufts of cotton glued to the wing surface near the wall junctions and also by means of

some auxiliary surface-pressure holes. These were all at the same chordwise position (their coordinates are listed in Table 3) and were connected to adjacent tubes in a bank of water manometers.

Flexing of the model under aerodynamic loads was limited by two straining wires attached through the lower surface to pivots on the axis of rotation (see Fig.1). The other ends of the wires were taken out through holes in the wall of the working section and fixed to the tunnel structure.

## 2.2 Data acquisition system

The differences between the surface pressures on the model and the surface pressure on the roof of the working section of the wind tunnel $p_r$, were measured by eight pressure transducers. These were installed in rotary Scanivalves, four for each of the two test areas of the model. Their outputs were passed through a digital voltmeter and transcribed to paper tape.

Each Scanivalve was capable of monitoring 48 pressure lines, but to overcome hysteresis problems with the transducers, alternate ports were connected to a constant pressure (7 $kN/m^2$) which exceeded the maximum surface pressure on the model. Of the remaining 24 ports, the first was used to determine the zero shift in the bridge circuit; the second measured the response of the transducer to an accurately known reference pressure (-17.20 $kN/m^2$) and the third measured the difference between the static pressure in the tunnel settling chamber and $p_r$, thus giving a measure of dynamic pressure.

Two of the transducers had a linear pressure range of ±34 $kN/m^2$ and were used to monitor the high suctions around the leading edge of the model. The other six transducers produced a linear output voltage over the range ±17 $kN/m^2$. The settling time for each pressure line was 0.35 s.

# 3 DESCRIPTION OF TESTS

## 3.1 Wind-tunnel runs

All the runs were carried out at a wind speed of 61 m/s, corresponding to a Reynolds number based on chord of $1.9 \times 10^6$. At some spanwise positions there was a slight discontinuity in the slope of the upper surface of the model at the junction of the leading edge and main assembly. Although transition was left free, it is possible that under some conditions, it was forced to occur at this junction.

Some preliminary runs were performed to determine the ranges of incidence within which the flow remained attached over the flaps. The upper surfaces of the flaps were tufted, together with the wing-root areas. Suction was applied to inhibit separation at the junctions with the tunnel roof and floor, and the angle of incidence increased until the flow separated over the flaps. For both flaps deflected $5^{\circ}$, separation was just apparent at the trailing edge at an angle of incidence of $6^{\circ}$ and with a suction pressure of $-3.4$ kN/m$^2$, corresponding to a pressure coefficient based on tunnel dynamic pressure of $-1.5$. With both flaps undeflected, a maximum angle of $10^{\circ}$ could be reached before the flow over the flaps began to separate. At $12^{\circ}$ the stall was intermittent with a suction pressure of $-21$ kN/m$^2$, i.e. a pressure coefficient of $-9.2$. A lowest angle of incidence of $-10^{\circ}$ was chosen.

The uniformity and two-dimensionality of the flow could be checked by reference to the auxiliary pressure tappings. Examples for three angles of incidence, with the flaps undeflected, are shown on Fig.3. Ignoring small differences, perhaps due to slight errors in the chordwise positions of the holes, the levels of pressure within two chords of the centreline appear to be uniform. There are departures from these levels at the extremes of the wing and there is an unexplained small difference in $C_p$ at the port end of the model at $\alpha = -10^{\circ}$. In general, however, it appears that the flow was two-dimensional over the areas of the wing used for the pressure-distribution surveys.

Two sections of the wing were scanned at each angle of incidence (or data point) and each data point was repeated before going on to the next angle. Four different configurations were tested: both flaps undeflected; port flap down $5^{\circ}$; both deflected $5^{\circ}$; starboard flap down $5^{\circ}$. Just under two thousand pressure distributions were recorded during the course of the experiment. The paper-tape records of the transducer outputs were converted to $C_p$-form by computer, sorted into tube order, the trailing-edge pressure estimated and the values stored on magnetic tape. The trailing-edge pressure was obtained from the mean of the extrapolations of the pressure distributions on the upper and lower surfaces of the flap to the trailing edge. These extrapolations were made on the basis of least-squares parabolae fitted to the pressures at the last five stations on both surfaces. In order to make the best prediction of pressure at the trailing edge, in accordance with statistical practice most weight was given to the stations closest to it. Strong bias towards these points was obtained by

using weights that varied like $(x/c)^6$, i.e. 1 at the trailing edge and approximately 0.5 at (x/c) = 0.9. The magnetic tape records were edited to remove errors due to blocked pressure holes, digital-voltmeter malfunctions, etc. and the pressure distributions integrated to obtain sectional normal-force coefficients. The method of integration[6] was to fit cubic curves between each pair of $C_p$ values so that the resulting pressure distribution had continuous slope (but not necessarily continuous curvature).

## 3.2 Corrections and accuracy

An estimate of the blockage[7] was made prior to the commencement of the tests (but excluding separated-flow blockage) which gave a correction to the dynamic pressure in the working section of:

$$q \text{ (corrected)} = 1.002 \times q \text{ (measured)} \quad .$$

The speed control of the wind tunnel was set to give a speed of 61.0 m/s and a corrected dynamic pressure of 2.278 kN/m$^2$, which could be maintained to an accuracy of 0.1%.

The pressure coefficient $C_p$ can be expressed as:

$$C_p = \frac{p - p_r}{q} + \frac{p_r - p_0}{q}$$

where $p$ = the static pressure on the surface of the model;

$p_r$ = the static pressure on the roof of the working section of the wind tunnel;

$p_0$ = the static pressure in the undisturbed stream.

The second term in this expression takes Mach number and blockage into account and was obtained from the standard tunnel calibrations. The Scanivalve transducers measured $(p - p_r)$, hence $C_p$ was obtained from the equation:

$$C_p = \frac{p - p_r}{2.278} + 0.1131 \quad .$$

Initial calibrations of the transducers indicated small amounts of non-linearity, so that the transfer functions could be expressed as:

$$p = \Pi \frac{v}{V} [1 + \varepsilon]$$

where $v$ = the output voltage corresponding to the pressure difference $p$;

$\Pi$ = a reference pressure producing output voltage $V$.

Experience suggested that the departures from linearity $\varepsilon$ could best be represented as cubic functions of $v/V$ such that $\varepsilon = 0$ at $v = 0,V$. Although these response voltages varied slightly from time to time and from scan to scan, they were sufficiently close to the calibration response for it to be safe to assume that the characteristics of the cubic functions $\varepsilon$ were unchanged. The manufacturers' stated accuracies for the transducers were ±0.25% of the full-scale voltages, but as these were rarely approached, the actual accuracies were likely to be worse.

### 3.3 Repeatability

Chordwise pressure distributions were obtained at two spanwise stations during each run. As there were more stations on the upper area than the lower (see Fig.1), it was convenient to take repeat measurements at the last station (row 15) on the starboard area. Sufficient runs were performed at each angle of incidence and for each configuration for the results to be analysed statistically.

At each chordwise position, the mean $C_p$ was obtained (using equal weights for each result), together with the standard deviation from the mean. As an example, Fig.4 shows the average chordwise pressure distribution on row 15 at $\alpha = 8^o$ with the starboard flap deflected $5^o$. It was obtained from 18 runs taken during two days of testing. In order to indicate the variance of the results visually, 95% confidence limits on the mean values are also drawn. These limits[8] show the repeatability or accuracy of any $C_p$ result: for a given chordwise position, the probability is 0.95 that the true $C_p$ lies within the two limits.

It is clear from the figure that the results in this example are highly accurate - it is extremely difficult to distinguish the three lines. On integrating the distributions to obtain the normal-force coefficients, the curve through the mean values yields $C_N = 1.0844$ and the curves through the upper and lower confidence limits yield 1.0842 and 1.0847, respectively. The lower confidence limit leads to a higher normal force as it assumes that the true $C_P$s are more positive than those on the limit. These numbers themselves cannot be used to define the accuracy of the integrated $C_N$ values. A better way is to integrate the individual distributions and to analyse these. Doing this for the data used to produce Fig.4 gives a mean $C_N$ of 1.0845 with standard deviation 0.0016. It is thus 95% probable that the true value of $C_N$ lies within the limits 1.0852 and 1.0838.

Fig.5 shows a second example, again with the starboard flap deflected, but at zero angle of incidence. For this case it is possible to distinguish the

three curves in the region $0.05 < x/c < 0.2$. This is the region on the upper surface of the model behind the leading edge where the pressures were measured by the 'coarser' $34kN/m^2$ transducers. Integration of the individual $C_p$ distributions gives a mean $C_N$ of 0.3952 with 95% confidence limits of 0.3966 and 0.3938.

It is important to note that these results are indicative of the overall reliability of the experiment to measure sectional normal force. All experimental errors are included (and have been assumed to be random): tunnel speed, angle-of-incidence setting, transducer and logging-system errors. Certain systematic errors such as local variations in the profile of the model and inaccuracies in drilling the surface-pressure holes, have not been quantified. It is these errors which are the likely cause of the small variations in $C_p$ along the model span, shown on Fig.3.

The decrease in 'resolution' when going from the 17 to the $34kN/m^2$ transducers is worth investigating further. Suppose that the transducer and logging-system errors are small enough for the digital-voltmeter output to be accurate to within one count. If this is so, then it might be expected that on average, the scale value would be one count too large for one third of the results, accurate for one third and one count too low for the remainder. For 18 runs, the expected standard deviation of the readings would then be 0.84 counts. Converting this to $C_p$ - form, the likely standard deviation of the results due to digital-voltmeter inaccuracies would be an average of 0.0035 for the three low-range transducers and 0.0135 for the high-range transducer. The measured standard deviations for the $C_p$ s at each tube on the upper surface are compared on Fig.6 with these values, for the two examples shown on Figs.4 and 5. For both the examples shown on the figure (which are typical), the measured standard deviations are for nearly every tube less than those likely to occur through a random one-count error in the output of the voltmeter.

## 4 RESULTS

In order to be able to assess properly the changes in the chordwise pressure distribution when crossing the discontinuity in flap deflection, it is important to know that the basic flow in the absence of the discontinuity was devoid of spanwise or three-dimensional effects. Figs.7 and 8 compare the distributions at two widely-spaced chordwise sections, for the flaps-up and flaps-down configurations, at an angle of incidence of $6^o$. Row 5 (see Table 2) is on the centreline of the wind tunnel and row 15 is the most extreme section,

1.28 chords to starboard. Both sections appear to have irregularities in the upper-surface contour at the junction of the leading edge and main-wing components. The distributions are almost identical except for the pressures on the upper surface of the main component. These small differencies in the distributions are sufficient to produce noticeable differencies in the normal-force coefficients. If the earlier discussion on repeatability is used as a guide, it can be expected that the values of $C_N$ will be accurate to within approximately ±0.001 with 95% confidence, so that a difference of more than 0.002 is significant at this level. For both flaps undeflected, $C_N$ at rows 5 and 15 is 0.7328 and 0.7349 respectively and for both flaps deflected, 0.9742 and 0.9775, respectively. Although it is reasonable to conclude from Figs.7 and 8 that the flow was sufficiently two-dimensional for the purposes of this experiment, there were local vagaries in the surface contour which generated small but significant variations in the coefficient of normal force.

The distributions shown on Figs.7 and 8 are typical for the flaps-up and flaps-deflected configurations. They differ in the extent of suction on the lower surface, the pressure at the trailing edge and the amount of suction on the upper surface in the region of the flap hinge. There is also, of course, a difference in area following from the general increase in circulation with flap deflection. It has been assumed in a linear theory[1,2] that the nature of the pressure distribution changes discontinuously across a discontinuity in flap deflection. In practice, it might be expected that the change would take place over a finite spanwise extent and in earlier experiments[3] on an unswept wing of aspect ratio 7, the change seemed to take place in a distance of about 30% of the chord. Some results from the present experiment are given on Fig.9 which shows a perspective plot of the pressure distributions measured on the port area when the starboard flap was deflected $5^{\circ}$ and the port flap was undeflected. For clarity, only one set of axes has been drawn, with origin on the leading edge at the flap-break section: the origins of the others are staggered across the figure on the inclined line at the positions indicated by the circle symbols. This line represents spanwise distance from the flap break and has been drawn with $\bar{y}/c$ increasing to port. The angle of incidence is $6^{\circ}$, so the distributions may be compared directly with those on Figs.7 and 8.

At row 11 (0.028 chords from the flap junction) there is a slight indication of a suction peak over the flap knuckle. In other respects, however, the distribution looks very much like that of Fig.7 and the trailing-edge pressure

coefficient is definitely positive. At the other stations there are no traces of the suction peak at the hinge. The effect of the discontinuity on the shape of the pressure distribution seems to have disappeared in a spanwise distance of about 5% of the chord from the flap junction.

The complementary situation is indicated on the next figure. This shows measurements of the chordwise pressure distributions to port of the flap-break section when the port flap was deflected and the starboard flap undeflected. In this case it is seen that the distributions quickly take up the shape of the typical distribution on a two-dimensional wing with a deflected flap, given on Fig.8. A similar conclusion can be reached from tests for which the model was at a lower angle of incidence: Figs.11 and 12 show some results for $\alpha = -6^{\circ}$. On these four figures, the distributions over the flap hinge are not so well defined at row 9 because of an extra blocked pressure hole, with the result that the curves are slightly flatter there than they should be.

With the flaps deflected unequally there was a difference in loading on the two parts of the model. This difference was 'lost' in the region of the flap discontinuity in the form of a concentration of trailing vorticity. This had the effect of producing a local downwash over the flapped portion of the model and an upwash over the unflapped part, thus smoothing out the difference in loading. The extent of the span over which this smoothing took place can be seen from Figs.13, 14 and 15 which show the complete set of integrated $C_N$ for $\alpha = -6^{\circ}$, 0 and $6^{\circ}$, respectively. Due to an error of manufacture, no useful information was obtained at row 1, $\bar{y}/c = -0.7222$. Full lines have been drawn through the experimental values and the dashed lines have been drawn on the assumption of symmetry about the flap junction, $\bar{y}/c = 0$. For equally deflected flaps, the lines have been drawn with $C_N$ constant at the appropriate average value. With unequal flap deflection, the cross-over point has been put on the flap junction at the mean of the $C_N$ for equally deflected flaps.

From the figures it is clear that, at $\alpha = -6^{\circ}$ and 0 in particular, $C_N$ was not constant across the span of the model when the flaps were both up or both deflected. The jump in $C_N$ at $\bar{y}/c = 0.7$, of the order of 0.02 at $\alpha = -6^{\circ}$, varied with angle of incidence and flap deflection so that it is unlikely that it can be explained entirely by small differences (which would have to be no more than $0.3^{\circ}$) in the angles of deflection of the two flaps. Figs.7 and 8 indicate that the upper-surface contours were not identical at all spanwise stations. Similar comparisons at lower lift coefficients show that

these differences in contour gave rise to proportionately larger differences in $C_N$ .

Figs.13 to 15 show that, although the change-over from a pressure distribution typical of a flapped aerofoil section to one without a flap occurred quickly (within a spanwise distance of 11% of the chord), the changes to the local circulation took place over a much greater spanwise extent. For the $5^o$ angle of deflection used in these experiments, the effect of the discontinuity was apparent at distances of more than one chord away from the flap junction. The figures also show estimated spanwise loadings near a discontinuity on a plain wing of aspect ratio 10, by a linear theory[1,2]. The results were scaled to match the measured flap effectivenesses and increments added to account for the effect of camber. The theoretical and experimental variations of $C_N$ with distance from the discontinuity agree very well.

The force coefficients shown on these figures have not been corrected for the constraint effects of the tunnel walls. With the flaps undeflected, the correction to angle of incidence[7] amounts to about $0.05^o$ and the decrement in lift to about 1%. With the flaps deflected differentially, the two parts of the model were in local airstreams at slightly differing angles relative to the tunnel walls. The additional correction to lift for a section with a deflected trailing-edge flap[7] is about 0.7%, an insignificant amount compared with the observed increments in $C_N$ due to flap deflection of 0.25 to 0.3.

Those parts of the flap in the neighbourhood of the discontinuity were clearly less effective in generating increments in lift. Fig.16 shows the variation of normal-force coefficient with angle of incidence at row 11 just to port of the flap break. The difference between the increment in $C_N$ achieved with both flaps deflected and that with only one deflected appears to be independent of angle of incidence. Fig.17 shows the situation at row 15 and it can be seen that, 1.28 chords to starboard of the flap junction, $C_N$ with the flap deflected was still only 78% of that when both flaps were deflected.

Row 11 was the station closest to the flap break and the one where the chordwise pressure distributions were most different from either of the fully two-dimensional distributions. On Figs.9 and 11 it is apparent that when the flaps were deflected differentially, there was a slight carry-over of the suction peak at the flap hinge at this station. However, these figures are not ideal for demonstrating the magnitudes of the modifications to the pressure distribution with both flaps up, produced by the presence of the discontinuity in angle of

flap deflection. These are better seen by comparing the distributions at the same value of $C_N$. With both flaps undeflected, the equivalent $C_N$ was achieved at a higher angle of incidence than with just the port flap deflected. Interpolating linearly between the data on Fig.16, an angle of incidence of $7.22^\circ$ is required to produce the same $C_N$ as when the starboard flap was deflected at $\alpha = 6^\circ$. A similar interpolation of the individual $C_p(x)$ data yields the comparison shown on Fig.18. An increase in leading-edge suction balances the difference in suction over the flap hinge. The lower-surface pressures are very similar and the extrapolated pressures at the trailing edge are identical. The complementary situation at row 11 with the port flap deflected is shown on Fig.19 and the comments are much the same.

## 5 CONCLUSIONS

The experiments reported here were designed to provide information about the pressures on the surface of a wing in the vicinity of a discontinuity in angle of flap deflection. In order to simplify the interpretation of the results, a two-dimensional model was used and techniques employed to ensure that uniform flow was achieved across the model span (except, of course, in the neighbourhood of the flap junction when the flaps were deflected differentially). It was found that, when the two flaps were deflected equally, there were small local variations in the flow across the span, probably due to slight departures from the true upper-surface contour. These local variations generated a small amount of scatter in the spanwise distributions of normal force, which became more noticeable with decreasing angle of incidence. Nevertheless, this scatter was not important and the flow could be considered sufficiently uniform for the purposes of the experiment.

At any spanwise station, the chordwise pressure distribution has two different characteristic forms, depending on whether the flaps are deflected or not. The experiment investigated the transition from one form to the other when traversing in the spanwise direction across the flap junction with the flaps deflected differentially. The transition in shape but not in amplitude appears to be complete in a spanwise distance of about 10% of the chord, irrespective of the angle of incidence. In an earlier experiment on a three-dimensional model[3], the transition from one characteristic form to the other took place in a distance of about 30% of the chord. However, in that case the flaps were deflected $20^\circ$ as opposed to the $5^\circ$ used in the present experiments. There is the suggestion, therefore, that the strength of the discontinuity influences the extent of the

region of change in the chordwise pressure distributions. It was originally intended to include angle of flap deflection as one of the independent variables but unfortunately, due to deficiences in the design and manufacture of the model, this could not be done. The question thus remains to be settled by further experimentation.

At a discontinuity in angle of flap deflection there is a change in the level of the spanwise loading. Going from the side with the higher loading to the other, this loss in loading is transferred to the wake with a concentration of trailing vorticity centred on the flap junction. The consequent modifications to the otherwise uniform spanwise distribution of downwash, in the neighbourhood of the discontinuity, smooth out the jump in the spanwise loading. In theory, it might be supposed that the influence of the concentrated vortex would decrease as the inverse of the distance from the discontinuity. That is, the spanwise loading would tend asymptotically to the uniform-loading values with increasing distance from the flap junction. In these experiments it was found that the smoothing process was still apparent at one chord distance away from the discontinuity in angle of flap deflection and closely followed theoretical estimates. In fact, at 0.94 chord distance, the local coefficient of normal force was less than 80% of what it would have been with no discontinuity. This result was not dependent on angle of incidence. However, the extent of the spanwise region over which the loading differs from the uniform-loading levels by more than a given amount, will depend on the strength of the concentrated trailing vortex springing from the flap junction. This in turn is likely to be proportional to the difference in angles of flap deflection so it is probable that, for differential flap deflections greater than $5^{\circ}$, the effect of the discontinuity will be apparent at still greater distances.

To further the investigation using larger flap angles would require remanufacture of the surface panels of the model to include longer lengths of surface-pressure tubes, extending to at least two chords distance from the flap junction. At the same time, if it were decided to retain the plain-hinged flaps, the boundary-layer control system would have to be extensively redesigned. This work is being considered.

## Table 1

### SECTION COORDINATES

| Upper surface | |
|---|---|
| x/c | z/c |
| 0.0000 | 0.0000 |
| 0.0008 | 0.0034 |
| 0.0035 | 0.0083 |
| 0.0071 | 0.0119 |
| 0.0109 | 0.0147 |
| 0.0148 | 0.0168 |
| 0.0203 | 0.0202 |
| 0.0299 | 0.0247 |
| 0.0395 | 0.0285 |
| 0.0493 | 0.0319 |
| 0.0697 | 0.0380 |
| 0.0896 | 0.0430 |
| 0.1091 | 0.0471 |
| 0.1295 | 0.0509 |
| 0.1405 | 0.0528 |
| 0.1503 | 0.0543 |
| 0.1703 | 0.0573 |
| 0.1904 | 0.0599 |
| 0.2104 | 0.0622 |
| 0.2498 | 0.0659 |
| 0.2896 | 0.0688 |
| 0.3299 | 0.0707 |
| 0.3698 | 0.0717 |
| 0.4099 | 0.0716 |
| 0.4499 | 0.0708 |
| 0.4901 | 0.0691 |
| 0.5299 | 0.0669 |
| 0.5699 | 0.0640 |
| 0.5899 | 0.0624 |
| 0.6099 | 0.0605 |
| 0.6296 | 0.0586 |
| 0.6499 | 0.0565 |
| 0.6698 | 0.0543 |
| 0.7290 | 0.0469 |
| 0.7715 | 0.0409 |
| 0.7910 | 0.0378 |
| 0.8113 | 0.0347 |
| 0.8515 | 0.0282 |
| 0.8918 | 0.0213 |
| 0.9315 | 0.0140 |
| 0.9713 | 0.0060 |
| 1.0000 | 0.0000 |

| Lower surface | |
|---|---|
| x/c | z/c |
| 0.0000 | 0.0000 |
| 0.0010 | -0.0045 |
| 0.0041 | -0.0090 |
| 0.0081 | -0.0121 |
| 0.0120 | -0.0143 |
| 0.0160 | -0.0162 |
| 0.0218 | -0.0186 |
| 0.0299 | -0.0215 |
| 0.0400 | -0.0246 |
| 0.0501 | -0.0275 |
| 0.0895 | -0.0371 |
| 0.1293 | -0.0451 |
| 0.1696 | -0.0518 |
| 0.2096 | -0.0573 |
| 0.2496 | -0.0616 |
| 0.2897 | -0.0647 |
| 0.3295 | -0.0666 |
| 0.3696 | -0.0675 |
| 0.4095 | -0.0672 |
| 0.4497 | -0.0653 |
| 0.4896 | -0.0621 |
| 0.5296 | -0.0579 |
| 0.5693 | -0.0531 |
| 0.6093 | -0.0477 |
| 0.6492 | -0.0419 |
| 0.7315 | -0.0311 |
| 0.7714 | -0.0256 |
| 0.8110 | -0.0204 |
| 0.8513 | -0.0154 |
| 0.8914 | -0.0108 |
| 0.9316 | -0.0066 |
| 0.9714 | -0.0034 |
| 1.0000 | 0.0000 |

Table 2

POSITIONS OF CHORDWISE ROWS OF PRESSURE HOLES

| Row | $\bar{y}/c$ |
|---|---|
| 1 | -0.7222 |
| 2 | -0.6111 |
| 3 | -0.5000 |
| 4 | -0.4167 |
| 5 | -0.3333 |
| 6 | -0.2500 |
| 7 | -0.1945 |
| 8 | -0.1389 |
| 9 | -0.0833 |
| 10 | -0.0556 |
| 11 | -0.0277 |
| 12 | 0.0 |
| 13 | 0.7222 |
| 14 | 0.8333 |
| 15 | 0.9444 |

Distance $\bar{y}$ measured from the flap break, positive to starboard

Table 3

COORDINATES OF AUXILIARY PRESSURE HOLES

| x/c | y/c | z/c |
|---|---|---|
| 0.6495 | ±0.6664 | 0.0567 |
| | ±1.8329 | |
| | ±2.3331 | |
| | ±2.4995 | |
| | ±2.6662 | |
| | ±2.8329 | |
| | ±2.9441 | |

Distance y measured from the tunnel centreline
The tunnel wall is at y/c = ±3.0000

## Symbols

| | |
|---|---|
| $c$ | wing chord |
| $C_N$ | normal-force coefficient |
| $C_p$ | pressure coefficient |
| $p$ | static pressure on the model surface |
| $p_0$ | static pressure in the undisturbed stream |
| $p_r$ | static pressure on the roof of the tunnel working section |
| $q$ | dynamic pressure |
| $v$ | transducer output voltage corresponding to $p$ |
| $V$ | transducer output voltage corresponding to $\Pi$ |
| $x$ | distance from leading edge, in the direction of the chord |
| $y$ | distance from tunnel centreline, positive to starboard |
| $\bar{y}$ | distance from flap junction, $y-c/3$ |
| $z$ | distance normal to chordal plane, upper surface positive |
| $\alpha$ | angle of incidence |
| $\varepsilon$ | departure from linearity of transducer response |
| $\Pi$ | reference pressure used to calibrate transducers |

## REFERENCES


| No. | Author | Title, etc. |
|---|---|---|
| 1 | J. McKie | The estimation of the loading on swept wings with extending chord flaps at subsonic speeds. ARC CP 1110 (1969) |
| 2 | J. McKie | Some modifications to the calculation method for wings with part-span extending-chord flaps given in RAE Technical Report 69034. ARC CP 1213 (1971) |
| 3 | J. McKie | Low-speed wind-tunnel tests on an unswept wing of aspect ratio 7 with plain part-span trailing-edge flaps. RAE Technical Memorandum Aero 1613 (ARC 35969) (1974) |
| 4 | D.N. Foster<br>H.P.A.H. Irwin<br>B.R. Williams | The two-dimensional flow around a slotted flap. ARC R & M 3681 (1970) |
| 5 | D.N. Foster<br>J.A. Lawford | Experimental attempts to obtain uniform loading over two-dimensional high-lift wings. RAE Technical Report 68283 (ARC 31098) (1968) |
| 6 | D.S. Woodward | Further work on the integration of closed loops specified only by discrete data points. RAE Technical Report 73177 (ARC 35368) (1974) |
| 7 | H.C. Garner<br>E.W.E. Rogers<br>W.E.A. Acum<br>E.C. Maskell | Subsonic wind tunnel wall corrections. AGARDograph 109 (1966) |
| 8 | J. McKie | On the application of certain statistical methods to wind-tunnel testing. RAE Technical Report 75018 (1975) |

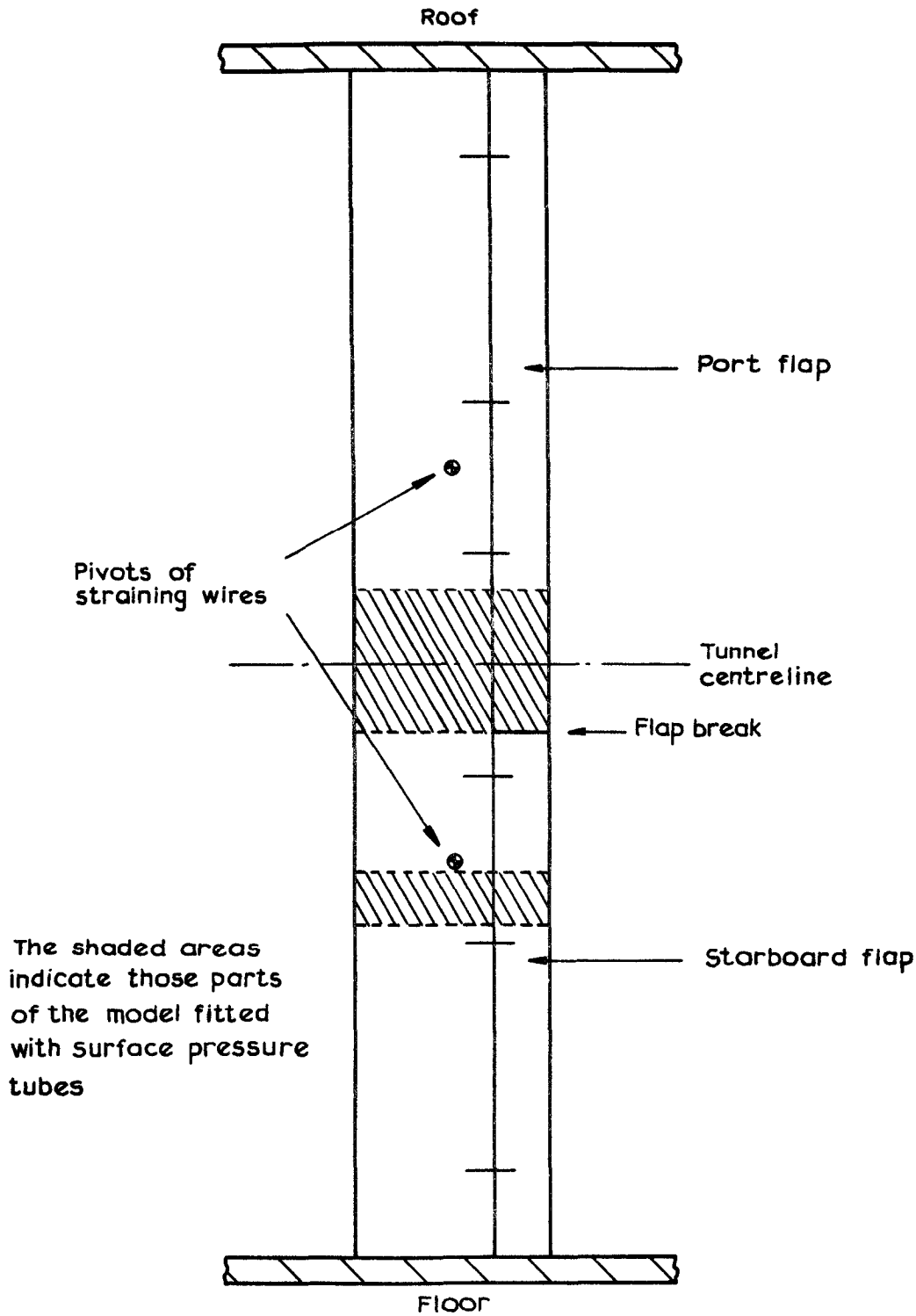


Fig. 1 Sketch of model mounted in wind tunnel

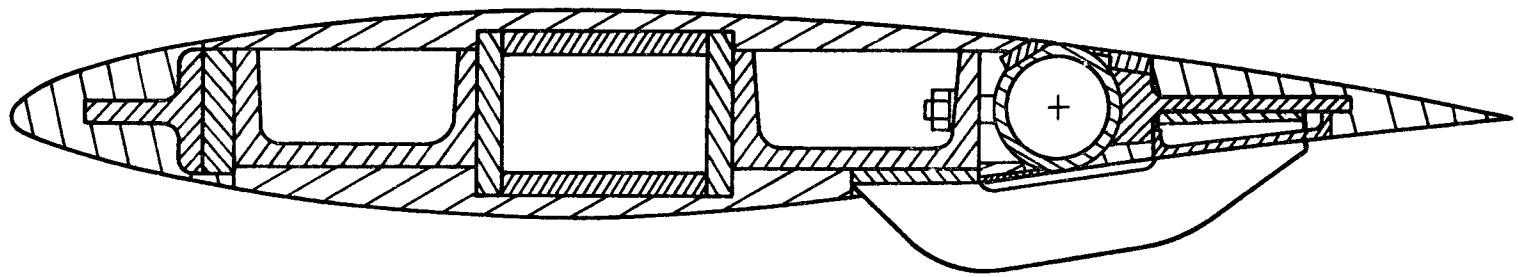

Typical section

Detailed part section showing method of attaching flap to wing (Flap deflected 5°)

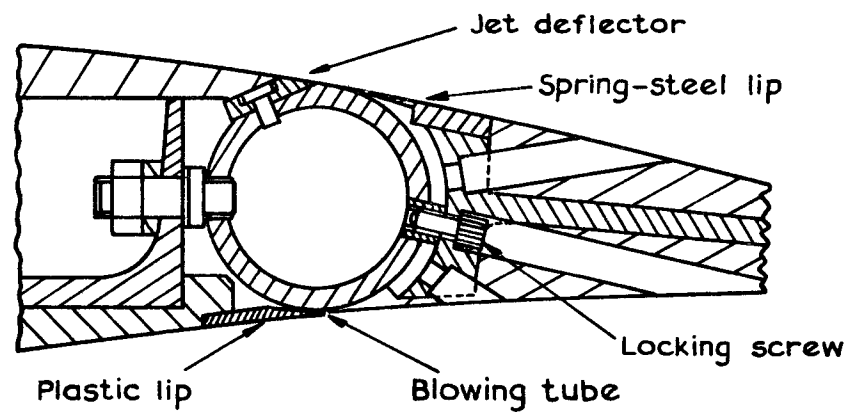


Fig. 2 Constructional details of aerofoil

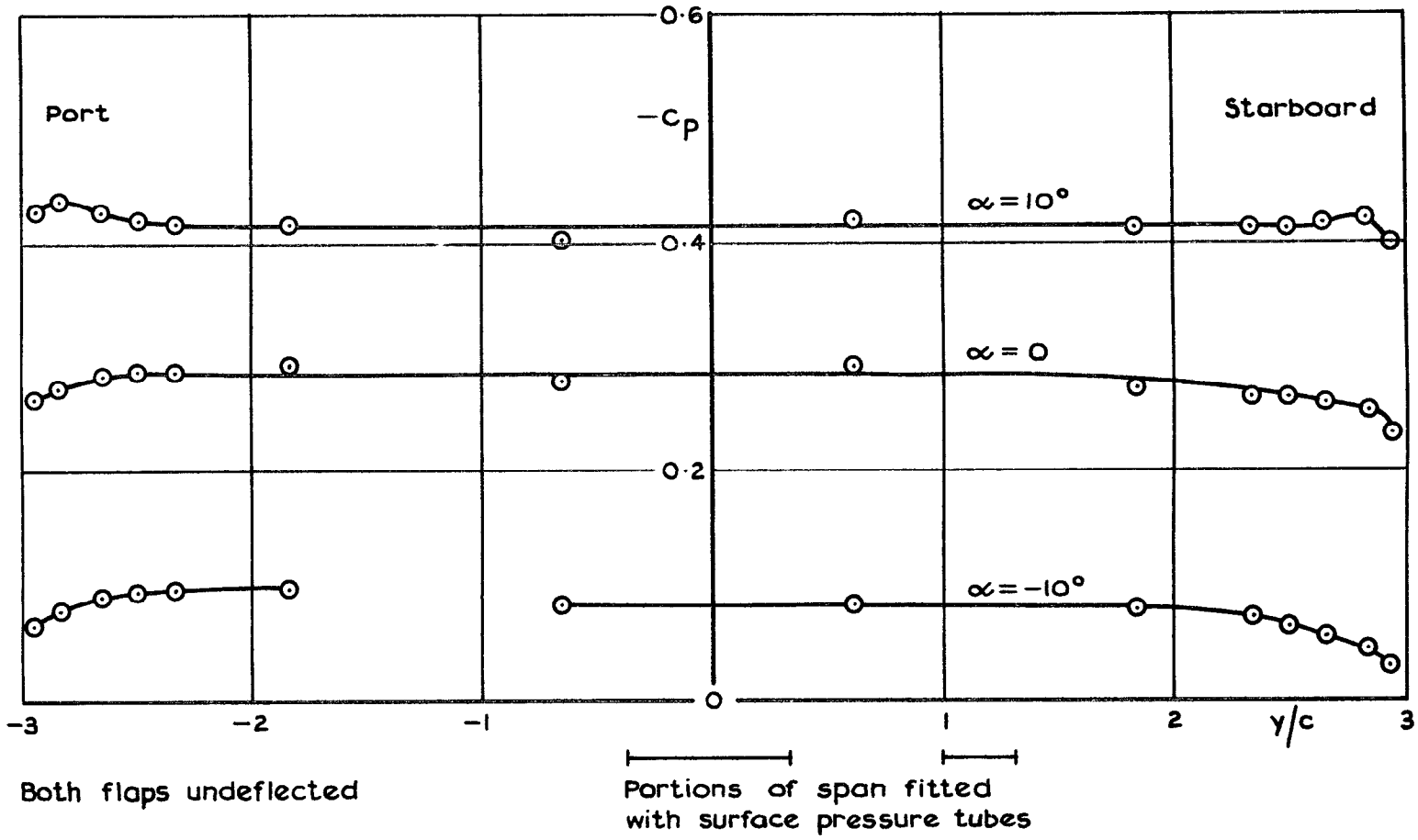


Fig. 3 Spanwise variation of pressure at one chordwise station

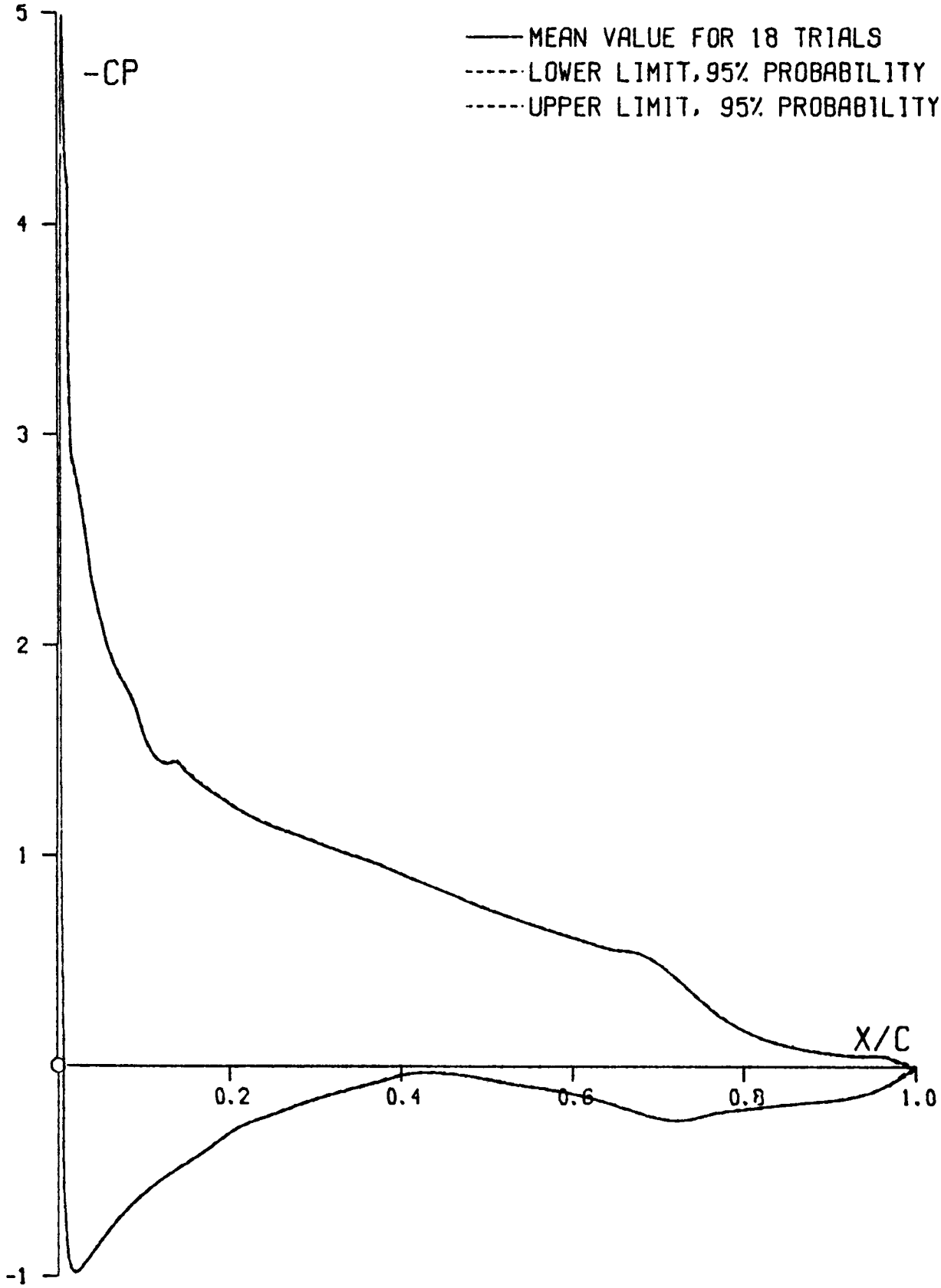


Fig.4 Average $C_p(x)$ at row 15. Starboard flap deflected. Alpha = $8^o$

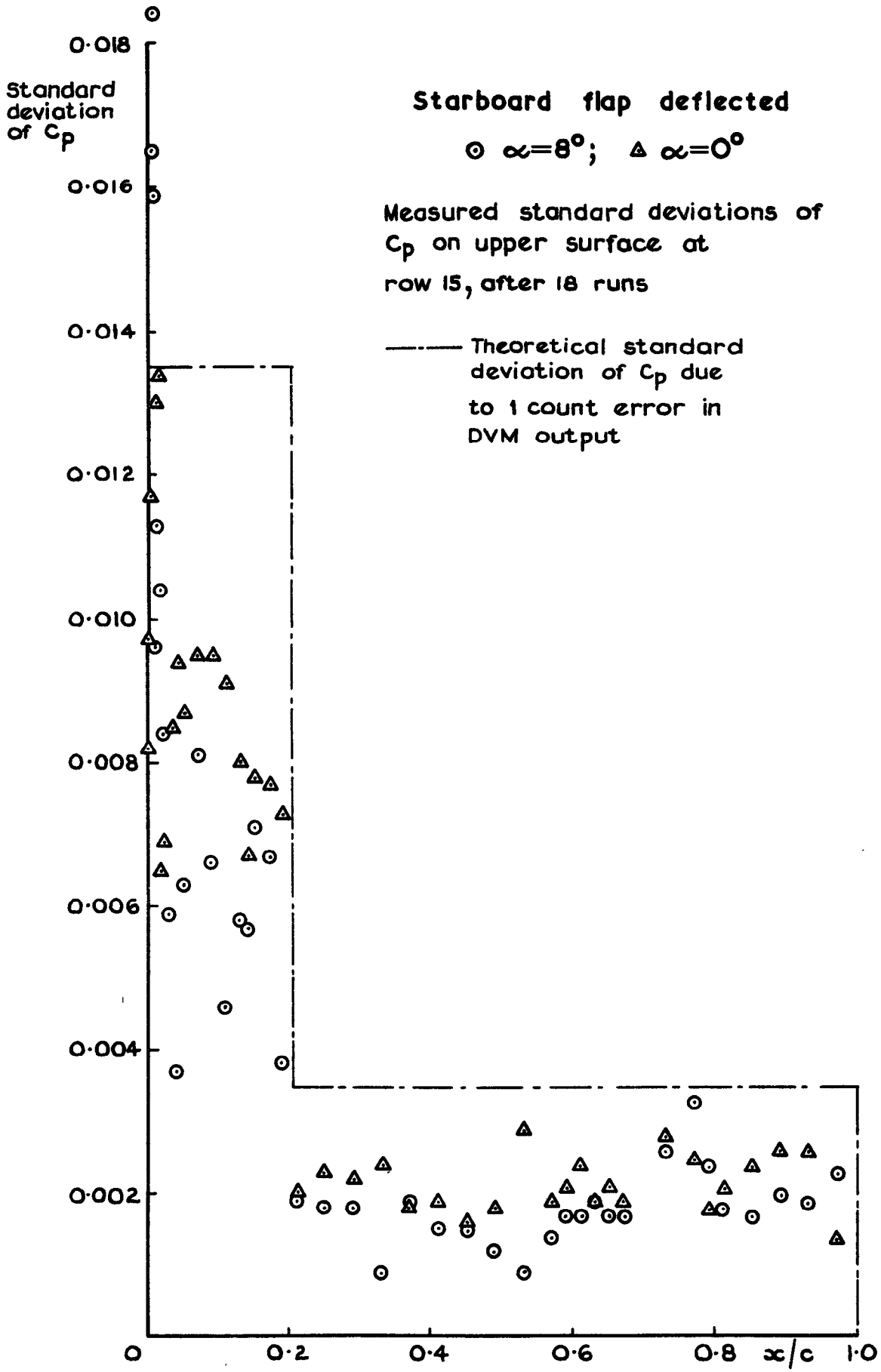


Fig.6 Chordwise variation of standard deviation of $C_p$

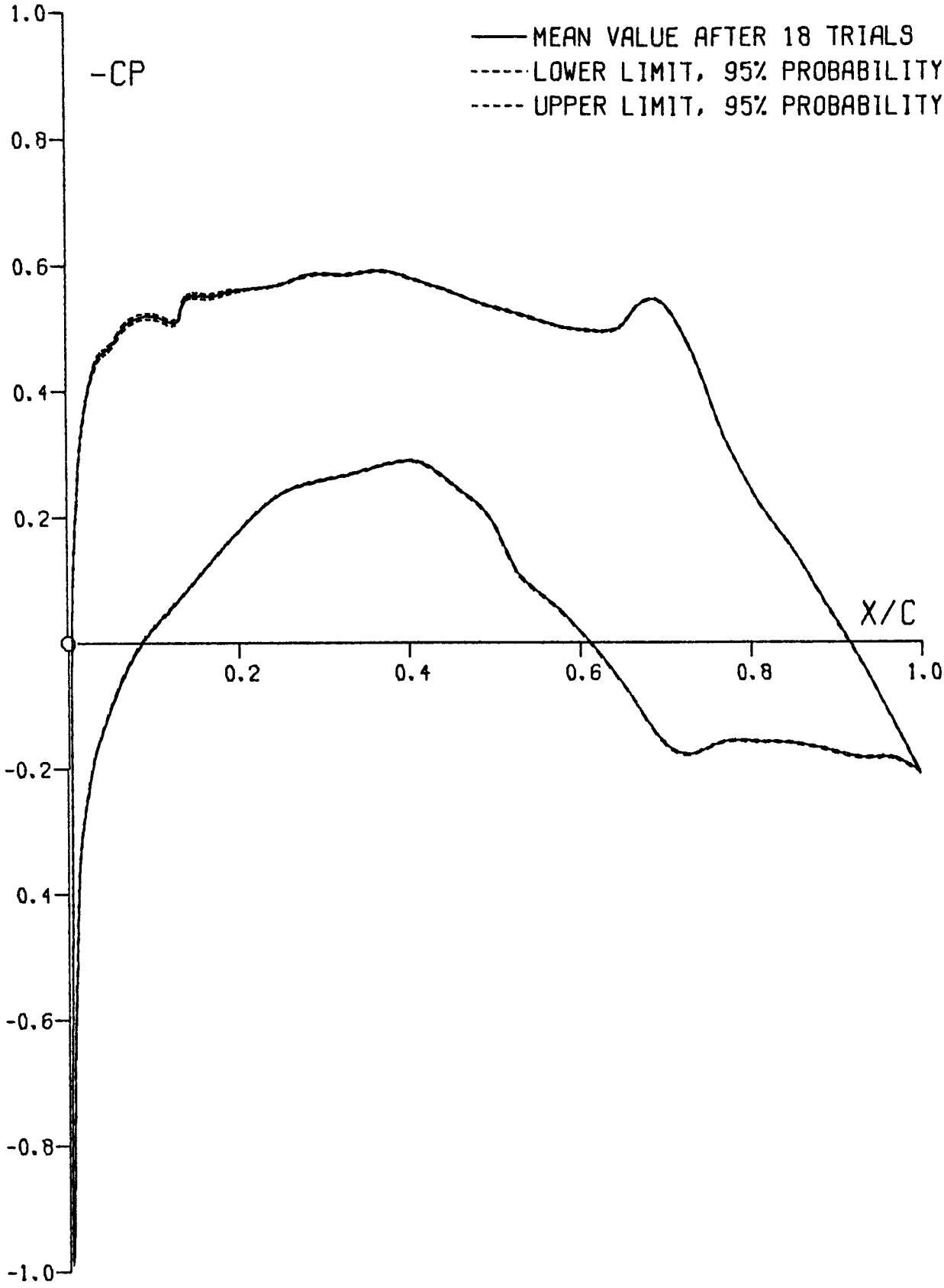


**Fig.5 Average $C_p(x)$ at row 15. Starboard flap deflected. Alpha = 0**

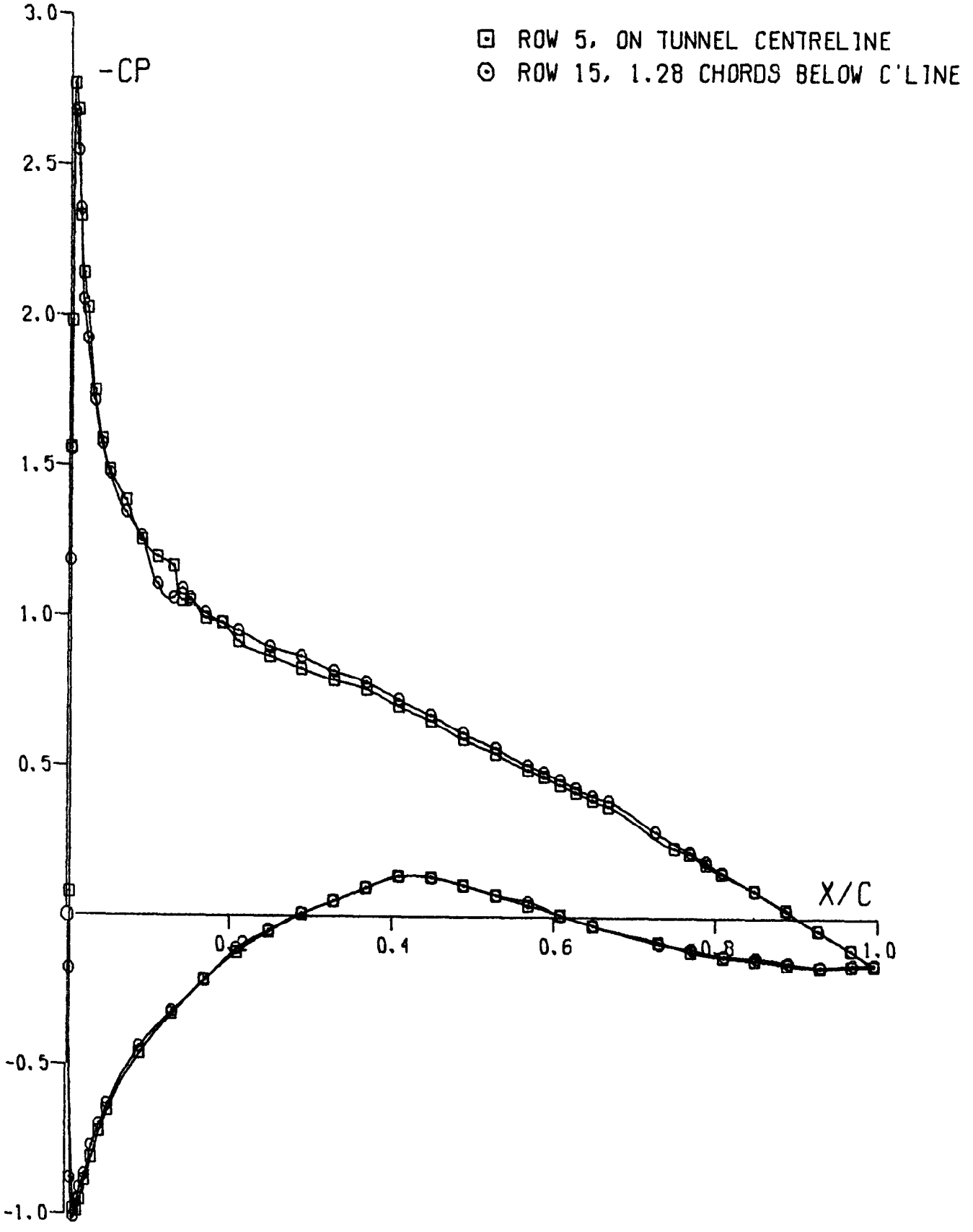


**Fig.7 Pressure distributions with both flaps undeflected. Alpha = 6°**

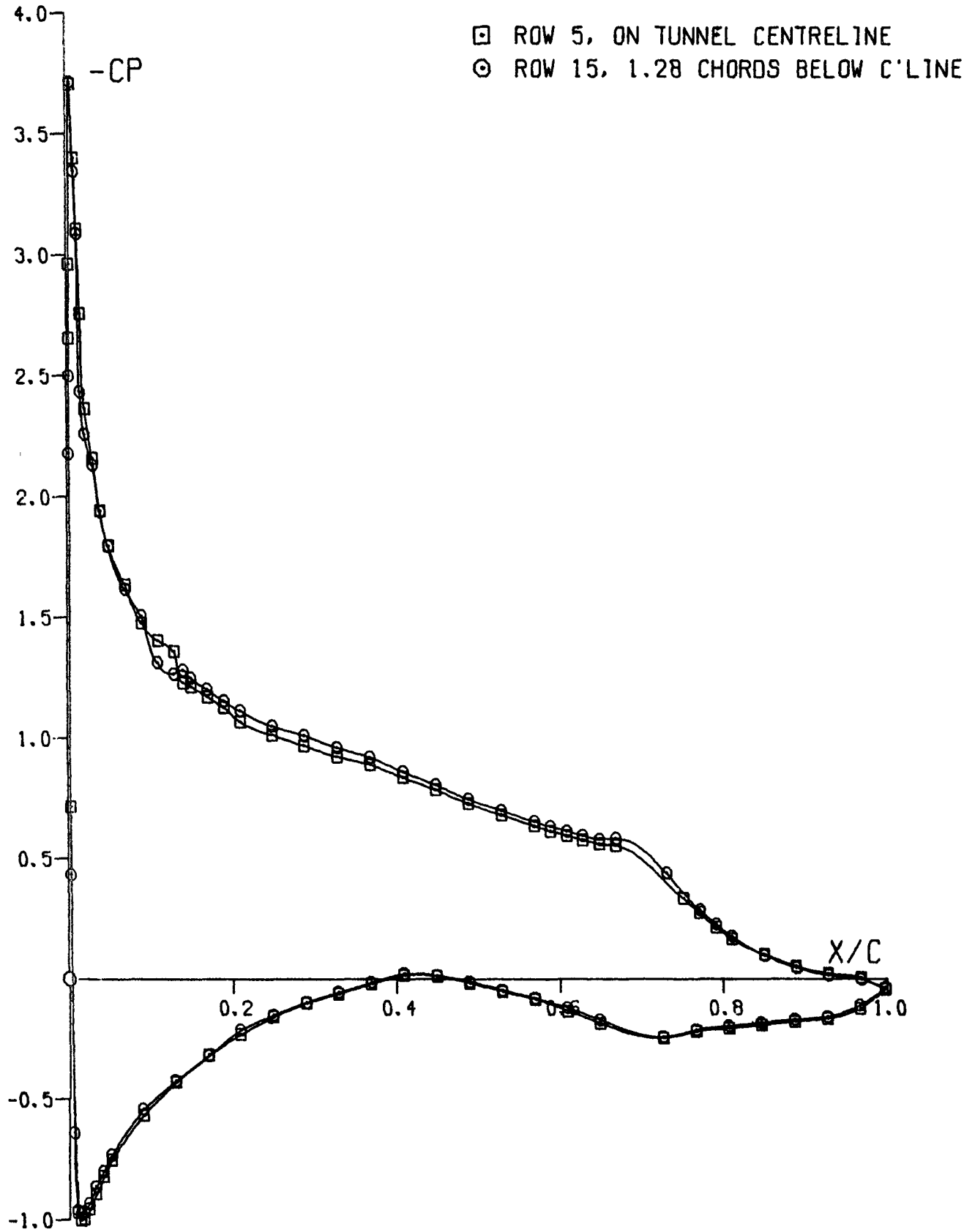


**Fig.8 Pressure distributions with both flaps deflected 5°. Alpha = 6°**

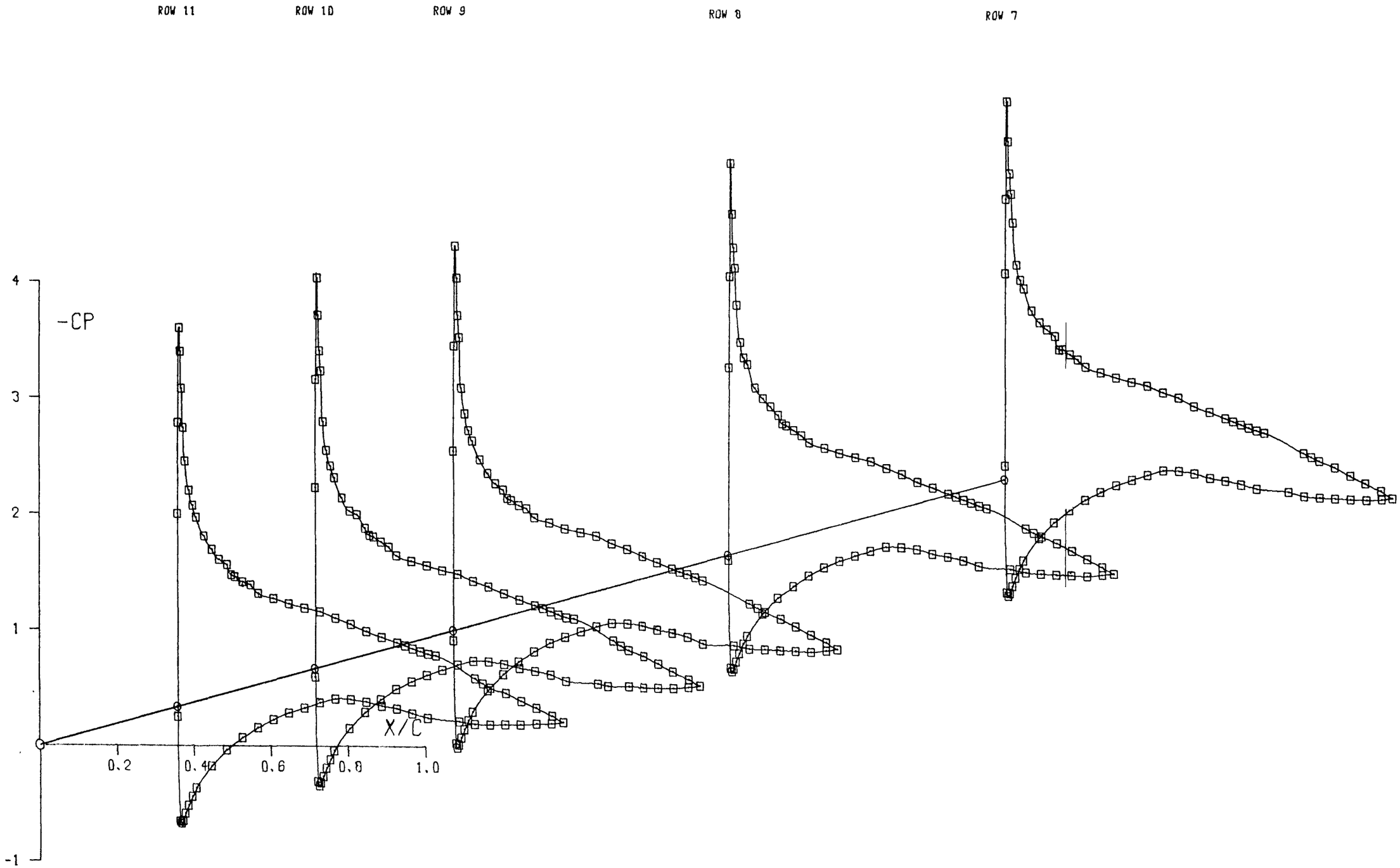


Fig.9 Change in $C_p(x)$ near flap discontinuity. Alpha = $6^o$, starboard flap deflected $5^o$

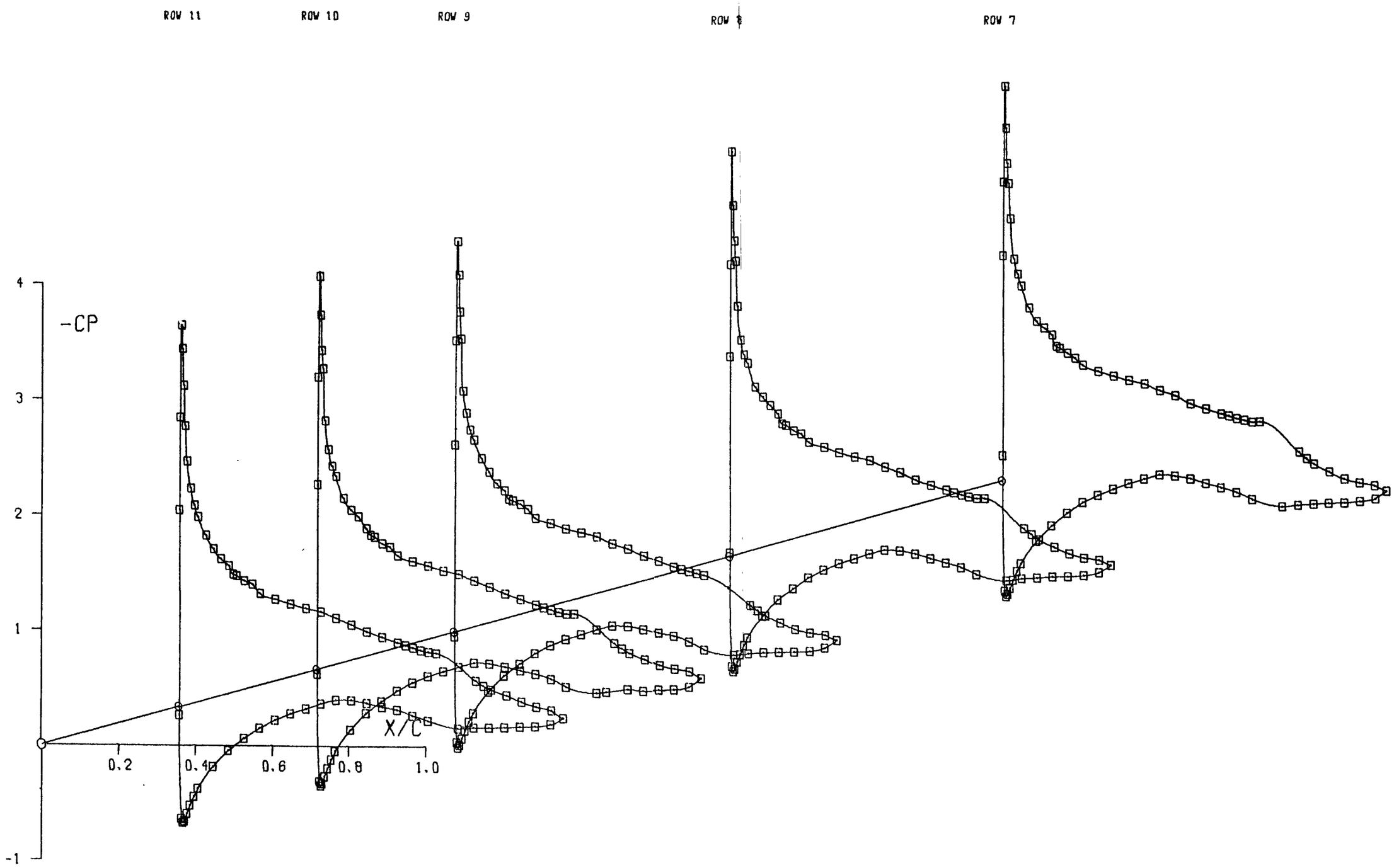


Fig.10 Change in $C_p(x)$ near flap discontinuity. Alpha = $6^o$, port flap deflected $5^o$

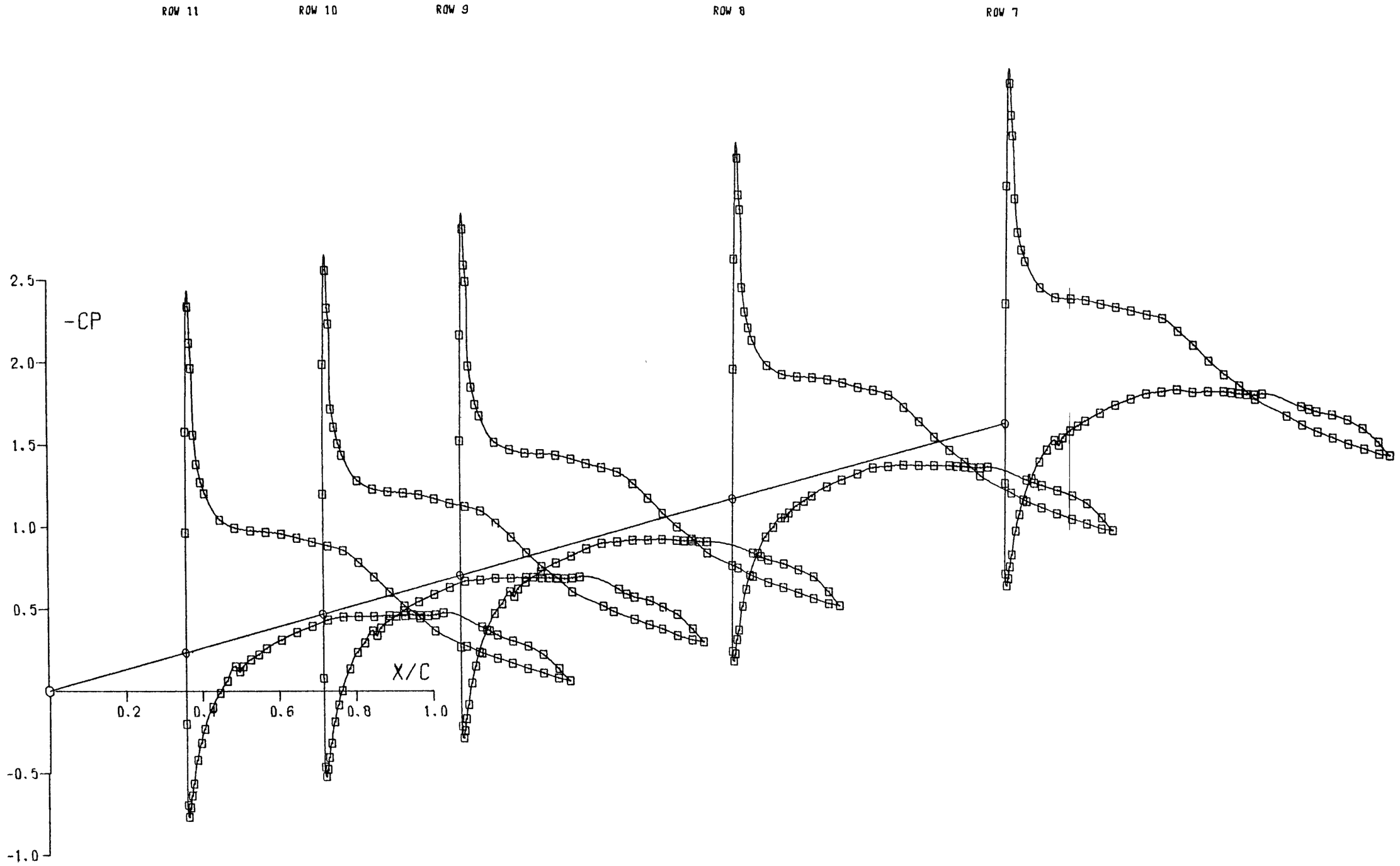


Fig.11 Change in $C_p(x)$ near flap discontinuity. Alpha = $6^o$, starboard flap deflected $5^o$

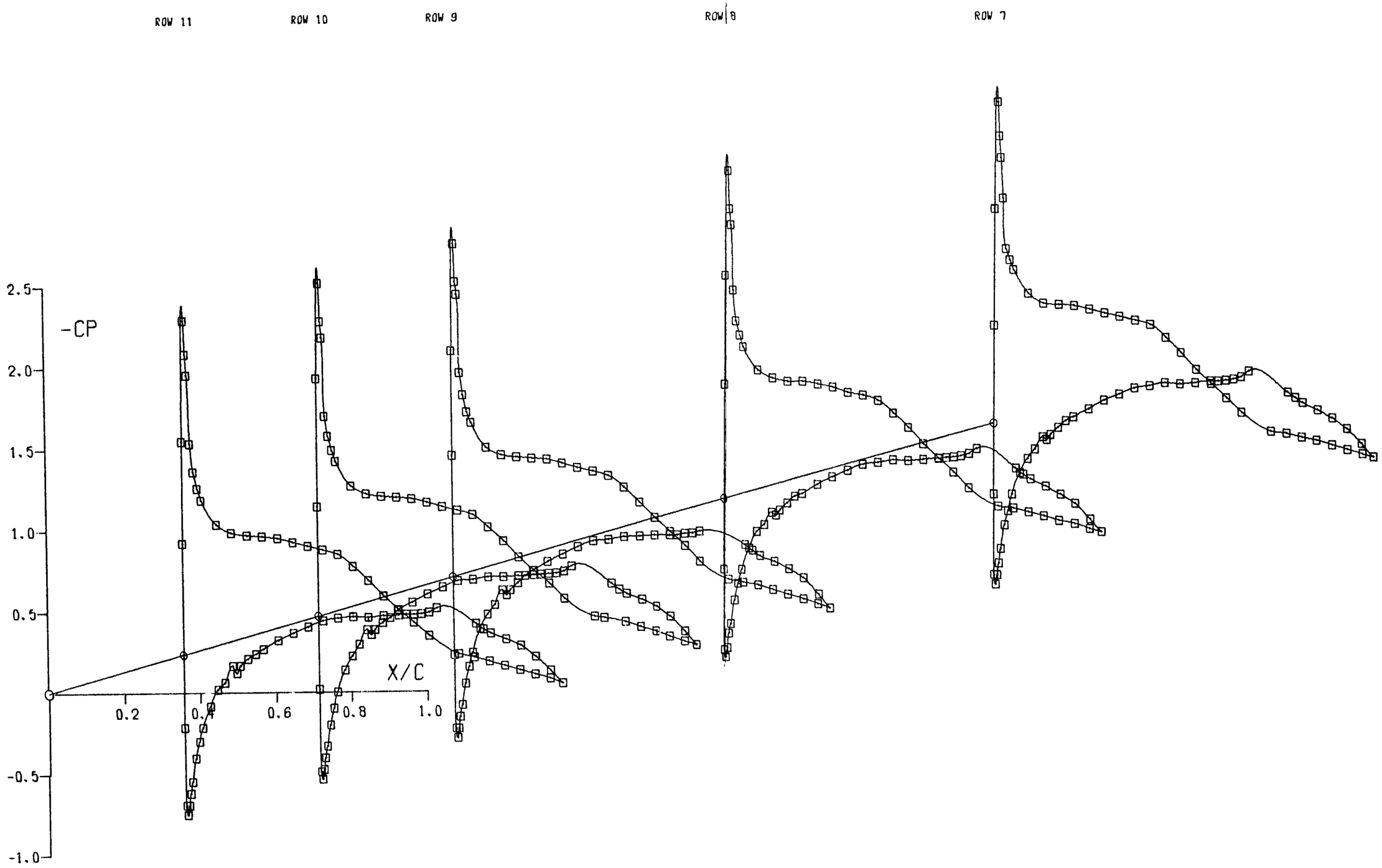


Fig.12 Change in $C_p(x)$ near flap discontinuity. Alpha = $6^o$, port flap deflected $5^o$

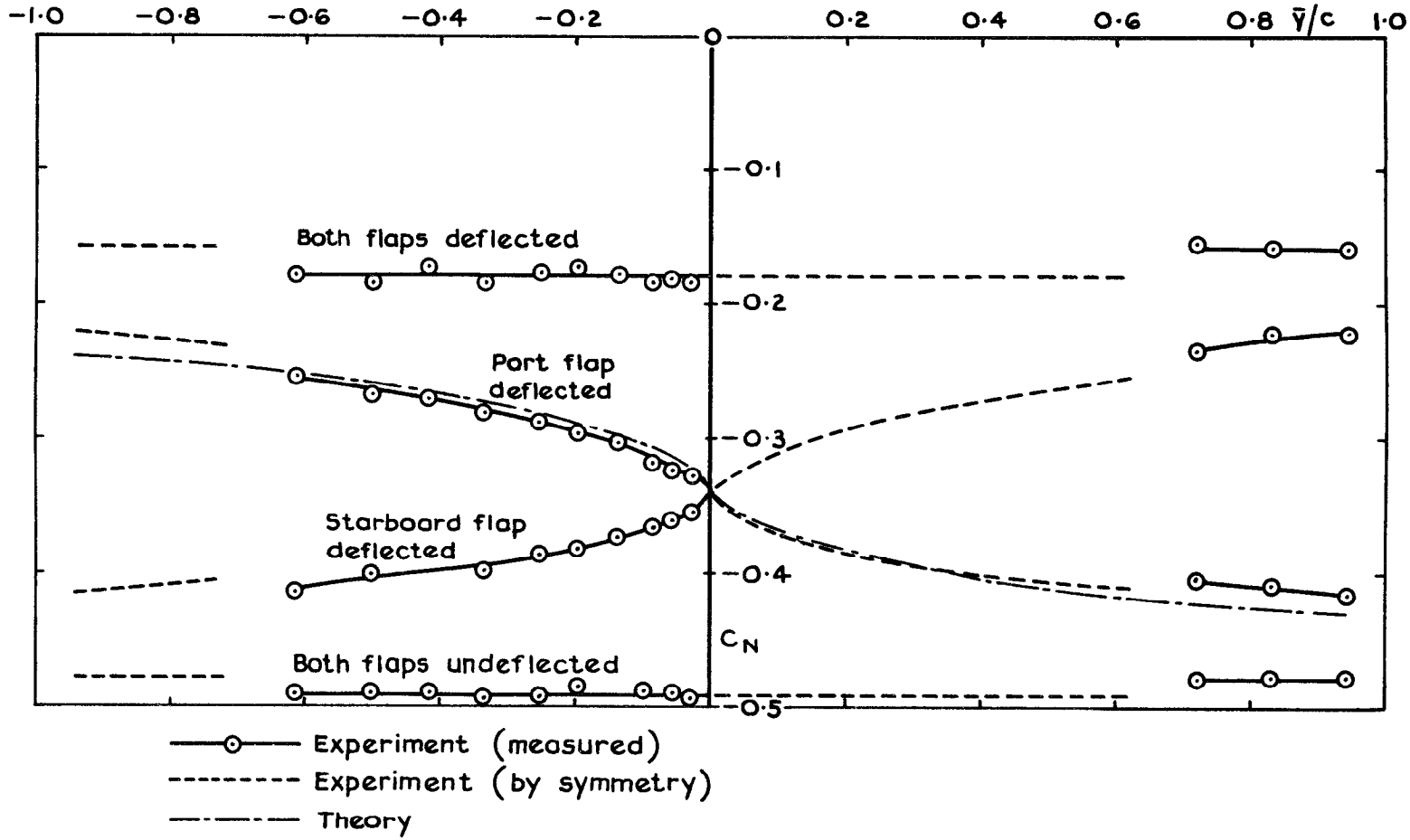


Fig. 13 Spanwise distributions of normal force coefficient. $\alpha = -6^{\circ}$

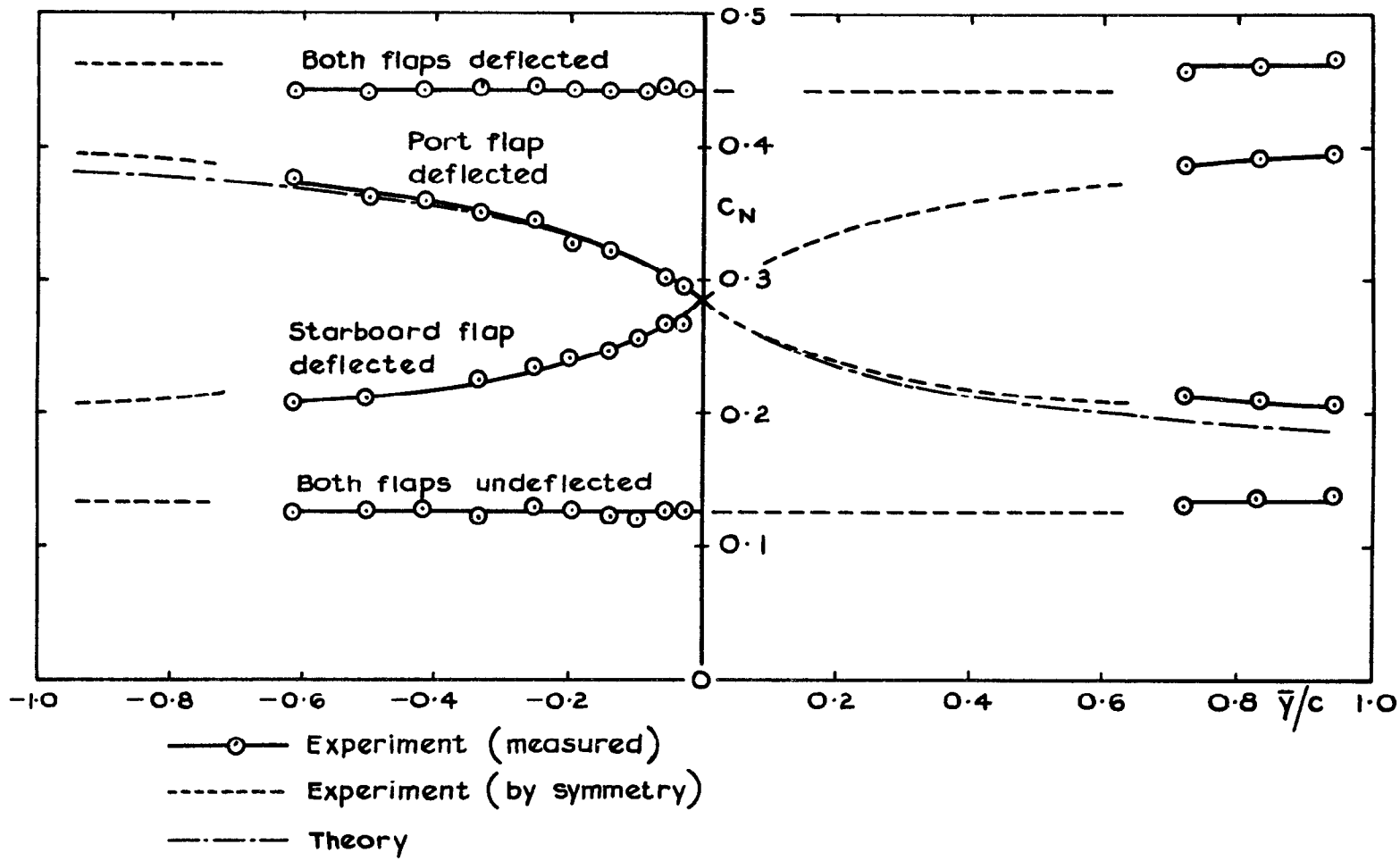


Fig. 14 Spanwise distributions of normal force coefficient. $\alpha = 0$

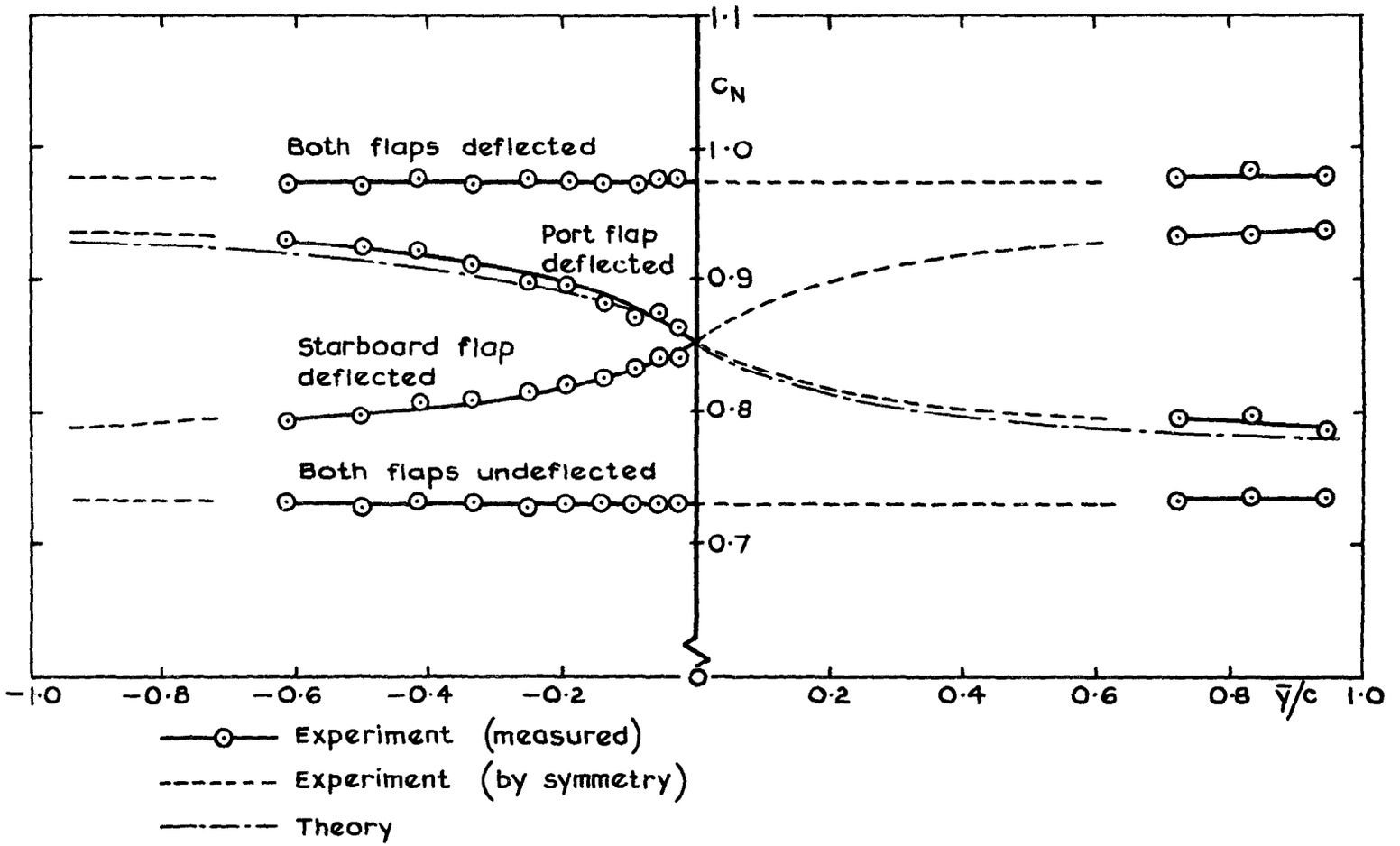


Fig. 15 Spanwise distributions of normal force coefficient. $\alpha = 6^\circ$

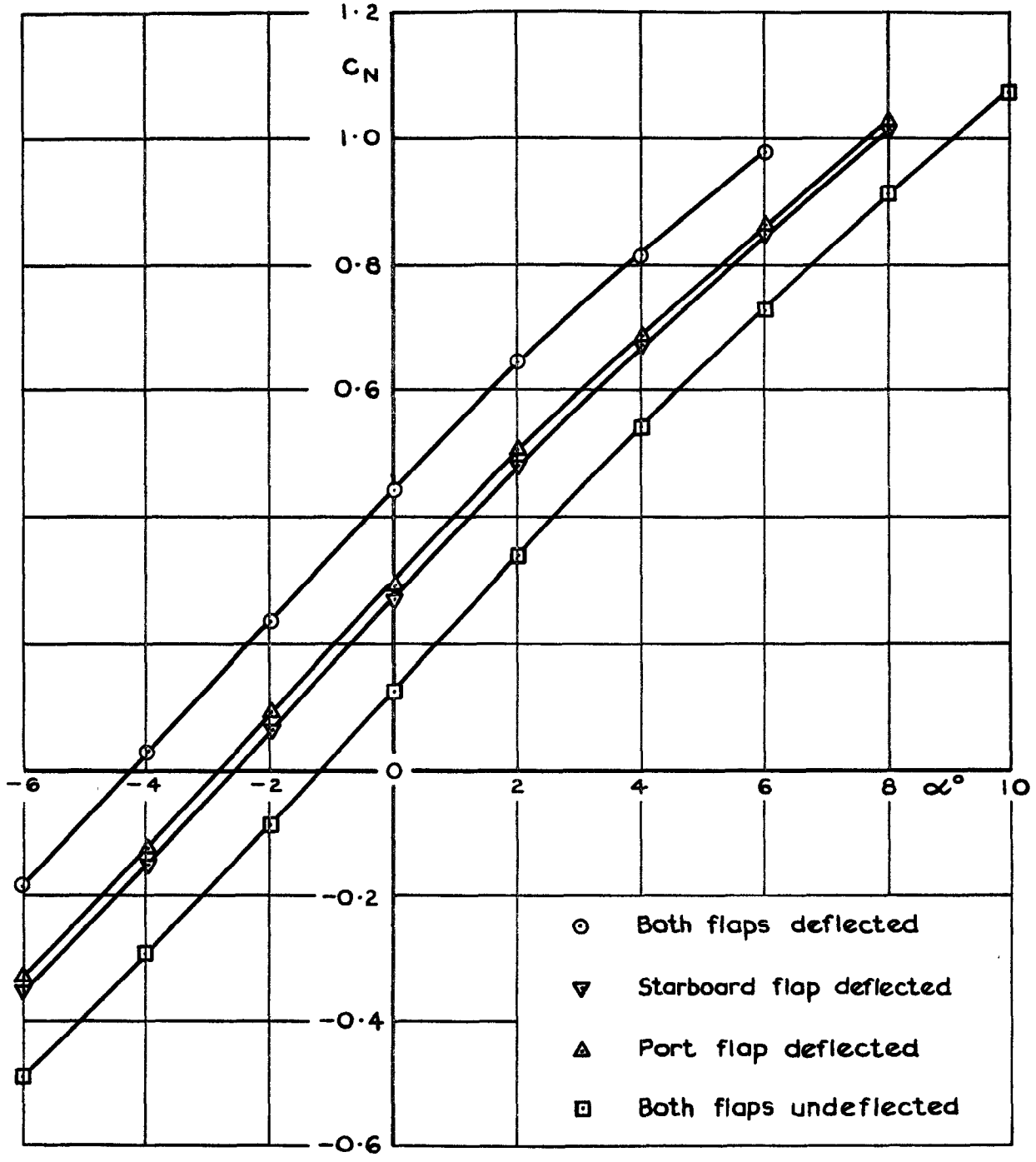


Fig. 16 Effect of incidence on sectional $C_N$ at row 11

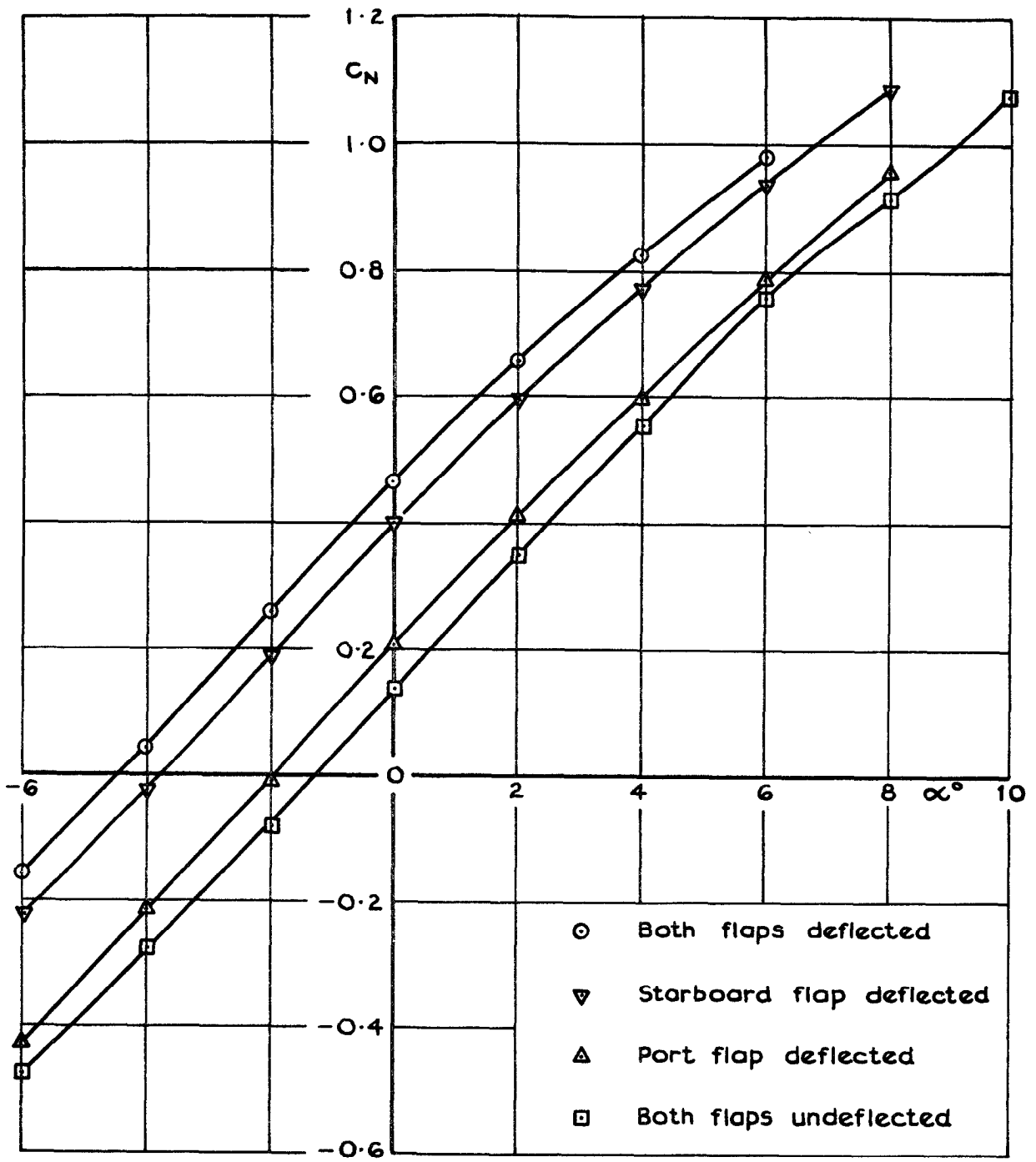


Fig. 17 Effect of incidence on sectional $C_N$ at row 15

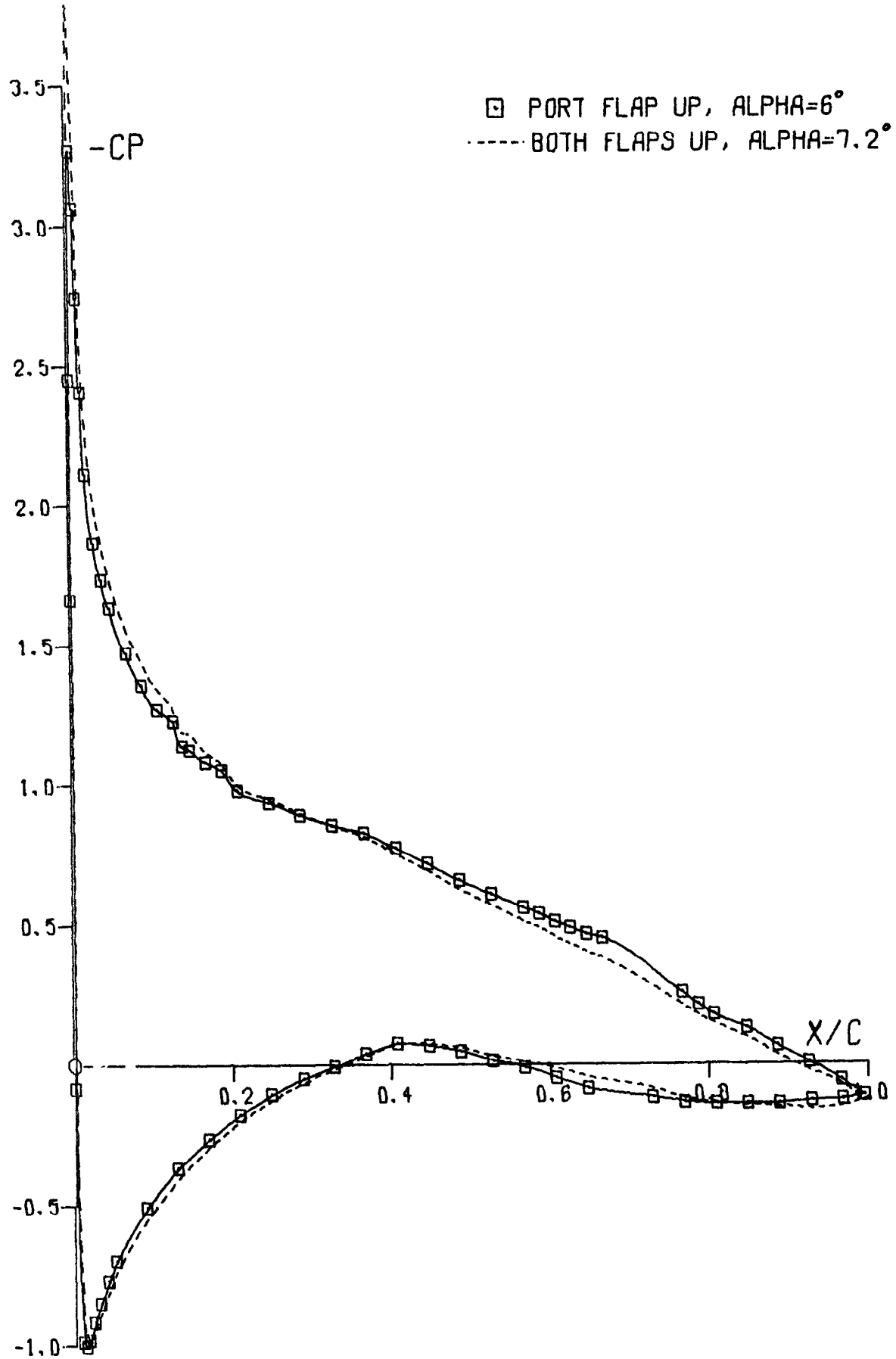


**Fig.18 Pressure distributions at a port station with flap up. Row 11, $C_N$ = 0.841**

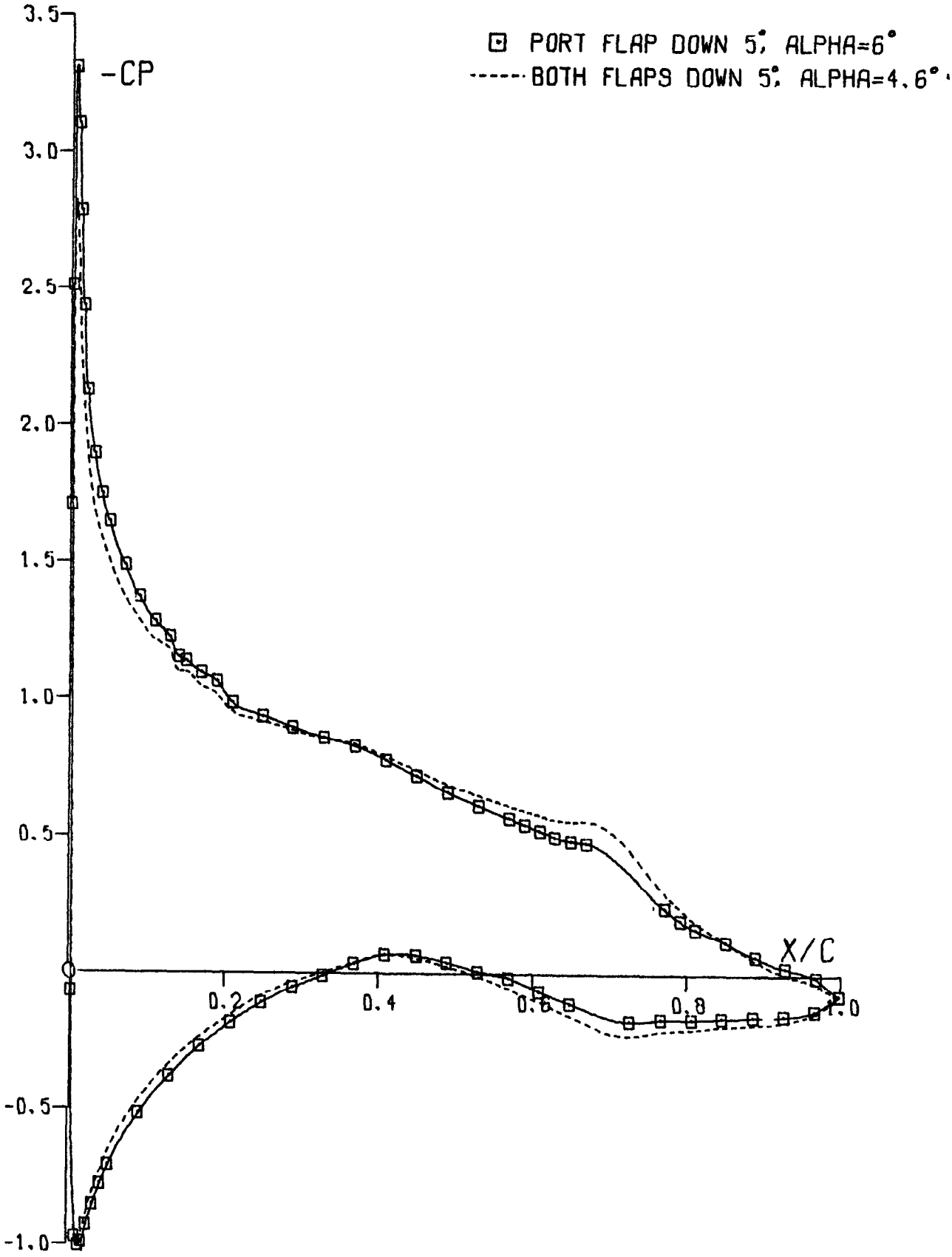


**Fig.19 Pressure distributions at a port station with flap down. Row 11, $C_N$ = 0.864**

*Printed in England for Her Majesty's Stationery Office by the Royal Aircraft Establishment, Farnborough. Dd. 289030 K4 8/75.*

ARC CP No.1326
December 1974

533.695.16 :
533.694.2 :
533.6.048.2

McKie, John

LOW-SPEED WIND-TUNNEL TESTS OF A TWO-DIMENSIONAL WING FITTED WITH TWO PLAIN, DIFFERENTIALLY-DEFLECTED, TRAILING-EDGE FLAPS

Chordwise pressure distributions were measured at several spanwise stations on a two-dimensional model wing fitted with a plain-hinged, trailing-edge flap, at a Reynolds number of $1.9 \times 10^6$ based on chord. The flap was divided into two parts and was deflected to a maximum of 5°. When the flaps were deflected differentially, the transition from a pressure distribution characteristic of the flaps-deflected configuration, to one characteristic of the flaps-up situation, took place within a spanwise distance of about 10% of the chord. This length was independent of the angle of incidence. Integrations for sectional normal force indicated, however, that modifications to the local circulation caused by a discontinuity in angle of flap deflection were apparent more than one chord distance away from the flap junction.

ARC CP No.1326
December 1974

533.695.16 :
533.694.2 :
533.6.048.2

McKie, John

LOW-SPEED WIND-TUNNEL TESTS OF A TWO-DIMENSIONAL WING FITTED WITH TWO PLAIN, DIFFERENTIALLY-DEFLECTED, TRAILING-EDGE FLAPS

Chordwise pressure distributions were measured at several spanwise stations on a two-dimensional model wing fitted with a plain-hinged, trailing-edge flap, at a Reynolds number of $1.9 \times 10^6$ based on chord. The flap was divided into two parts and was deflected to a maximum of 5°. When the flaps were deflected differentially, the transition from a pressure distribution characteristic of the flaps-deflected configuration, to one characteristic of the flaps-up situation, took place within a spanwise distance of about 10% of the chord. This length was independent of the angle of incidence. Integrations for sectional normal force indicated, however, that modifications to the local circulation caused by a discontinuity in angle of flap deflection were apparent more than one chord distance away from the flap junction.

These abstract cards are inserted in Technical Reports for the convenience of Librarians and others who need to maintain an Information Index.

*Cut here*

ARC CP No.1326
December 1974

533.695.16 :
533.694.2 :
533.6.048.2

McKie, John

LOW-SPEED WIND-TUNNEL TESTS OF A TWO-DIMENSIONAL WING FITTED WITH TWO PLAIN, DIFFERENTIALLY-DEFLECTED, TRAILING-EDGE FLAPS

Chordwise pressure distributions were measured at several spanwise stations on a two-dimensional model wing fitted with a plain-hinged, trailing-edge flap, at a Reynolds number of $1.9 \times 10^6$ based on chord. The flap was divided into two parts and was deflected to a maximum of 5°. When the flaps were deflected differentially, the transition from a pressure distribution characteristic of the flaps-deflected configuration, to one characteristic of the flaps-up situation, took place within a spanwise distance of about 10% of the chord. This length was independent of the angle of incidence. Integrations for sectional normal force indicated, however, that modifications to the local circulation caused by a discontinuity in angle of flap deflection were apparent more than one chord distance away from the flap junction.

*Cut here*

ARC CP No.1326
December 1974

533.695.16 :
533.694.2 :
533.6.048.2

McKie, John

LOW-SPEED WIND-TUNNEL TESTS OF A TWO-DIMENSIONAL WING FITTED WITH TWO PLAIN, DIFFERENTIALLY-DEFLECTED, TRAILING-EDGE FLAPS

Chordwise pressure distributions were measured at several spanwise stations on a two-dimensional model wing fitted with a plain-hinged, trailing-edge flap, at a Reynolds number of $1.9 \times 10^6$ based on chord. The flap was divided into two parts and was deflected to a maximum of 5°. When the flaps were deflected differentially, the transition from a pressure distribution characteristic of the flaps-deflected configuration, to one characteristic of the flaps-up situation, took place within a spanwise distance of about 10% of the chord. This length was independent of the angle of incidence. Integrations for sectional normal force indicated, however, that modifications to the local circulation caused by a discontinuity in angle of flap deflection were apparent more than one chord distance away from the flap junction.

DETACHABLE ABSTRACT CARDS

DETACHABLE ABSTRACT CARDS

Published by
HER MAJESTY'S STATIONERY OFFICE

*Government Bookshops*
49 High Holborn, London WC1V 6HB
13a Castle Street, Edinburgh EH2 3AR
41 The Hayes, Cardiff CF1 1JW
Brazennose Street, Manchester M60 8AS
Southey House, Wine Street, Bristol BS1 2BQ
258 Broad Street, Birmingham B1 2HE
80 Chichester Street, Belfast BT1 4JY
*Government Publications are also available through booksellers*

C.P. No. 1326

ISBN 011 470936 X